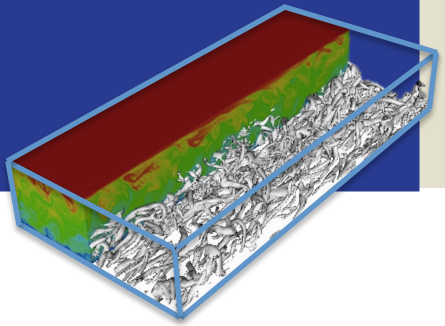

Multiphase Flow Laboratory
University of Udine

Collective particle dynamics in turbulent flows

Cristian Marchioli
University of Udine & CISM

Wien 11-13 February 2020

COMETE

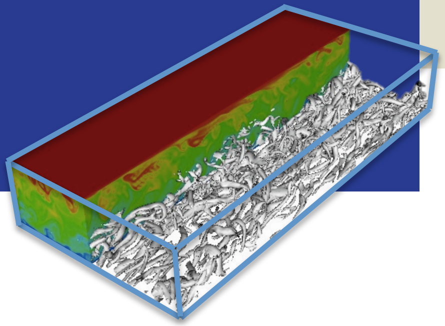

Euler-Lagrange description of particle-laden turbulent flows

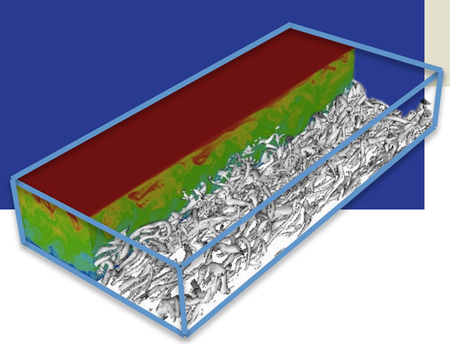

Eulerian vs Lagrangian Modelling

Eulerian Approach:

Focus on control volume

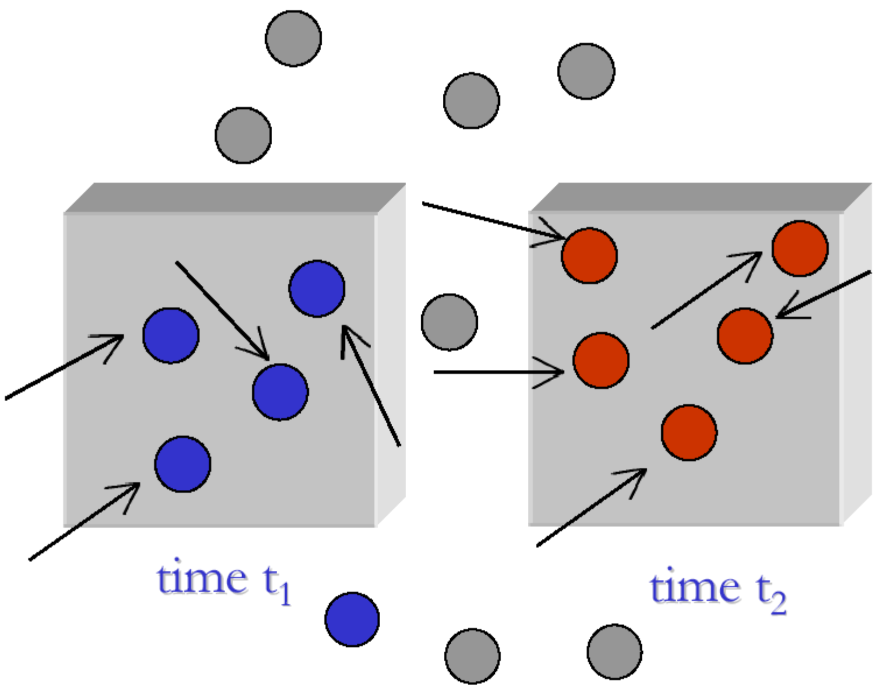

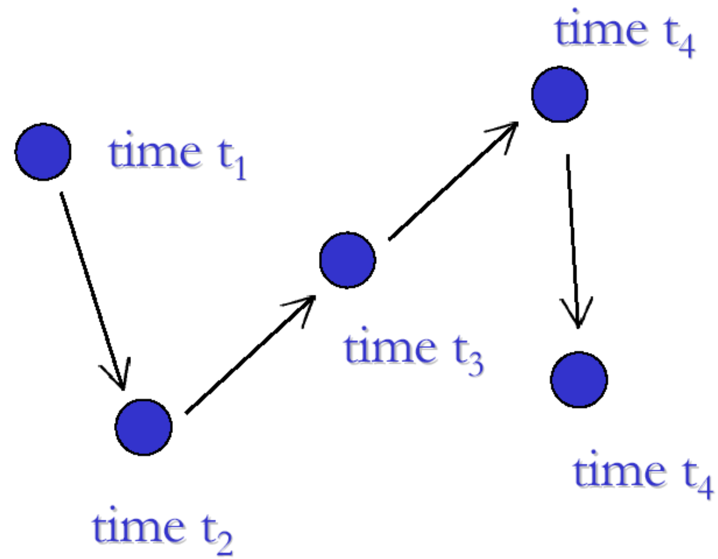

Lagrangian Approach:

Focus on particle trajectory

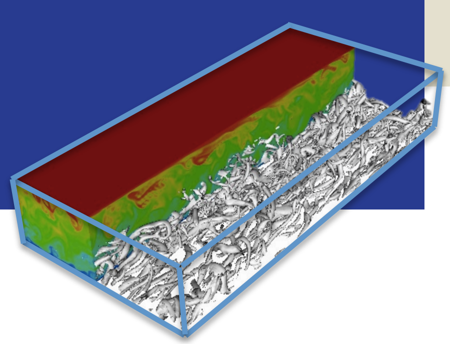

Eulerian vs Lagrangian Modelling

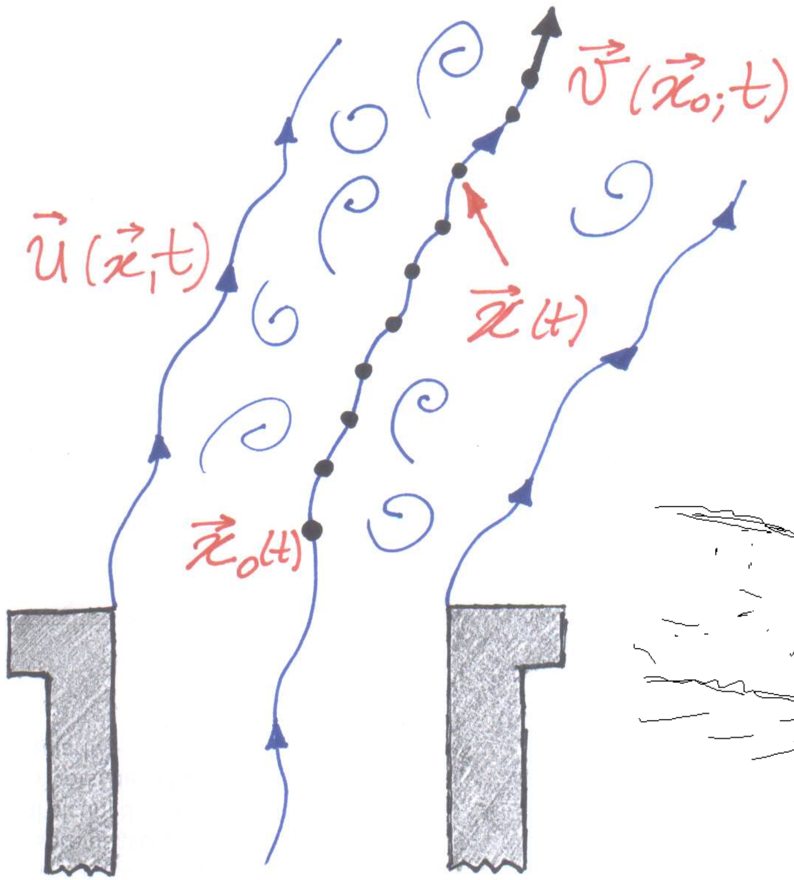

<u>Eulerian approach</u>: Focus is on the velocity at fixed control volumes points in the flow where one sees different particles at a time.

<u>Lagrangian approach</u>: Focus is on individual fluid particles, followed along their trajectory.

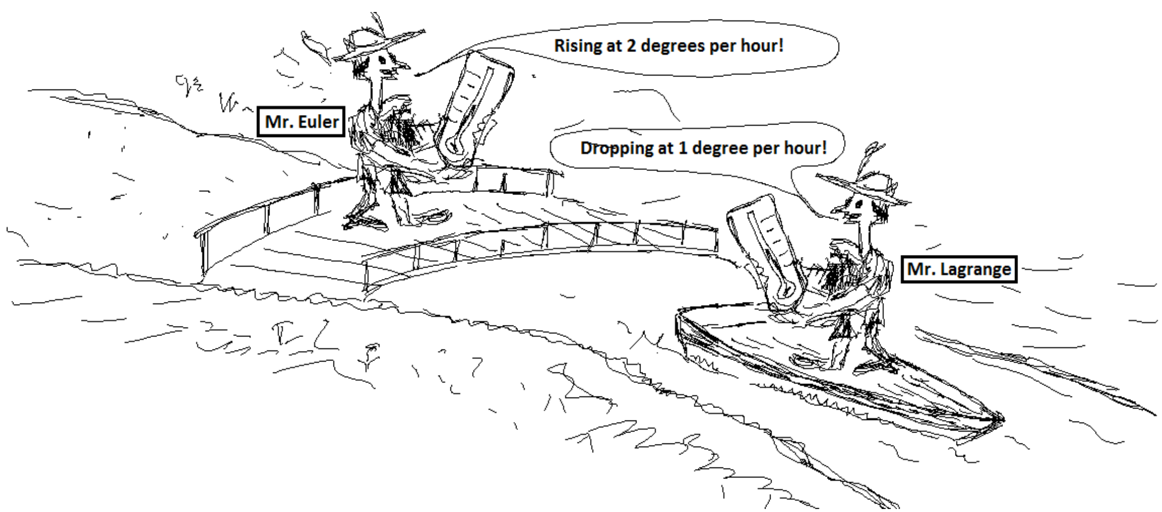

www.flowillustrator.com

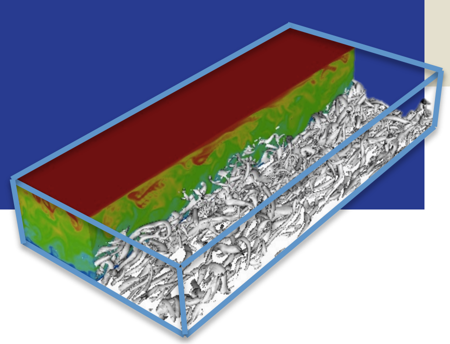

Main approaches to the numerical simulation of turbulence

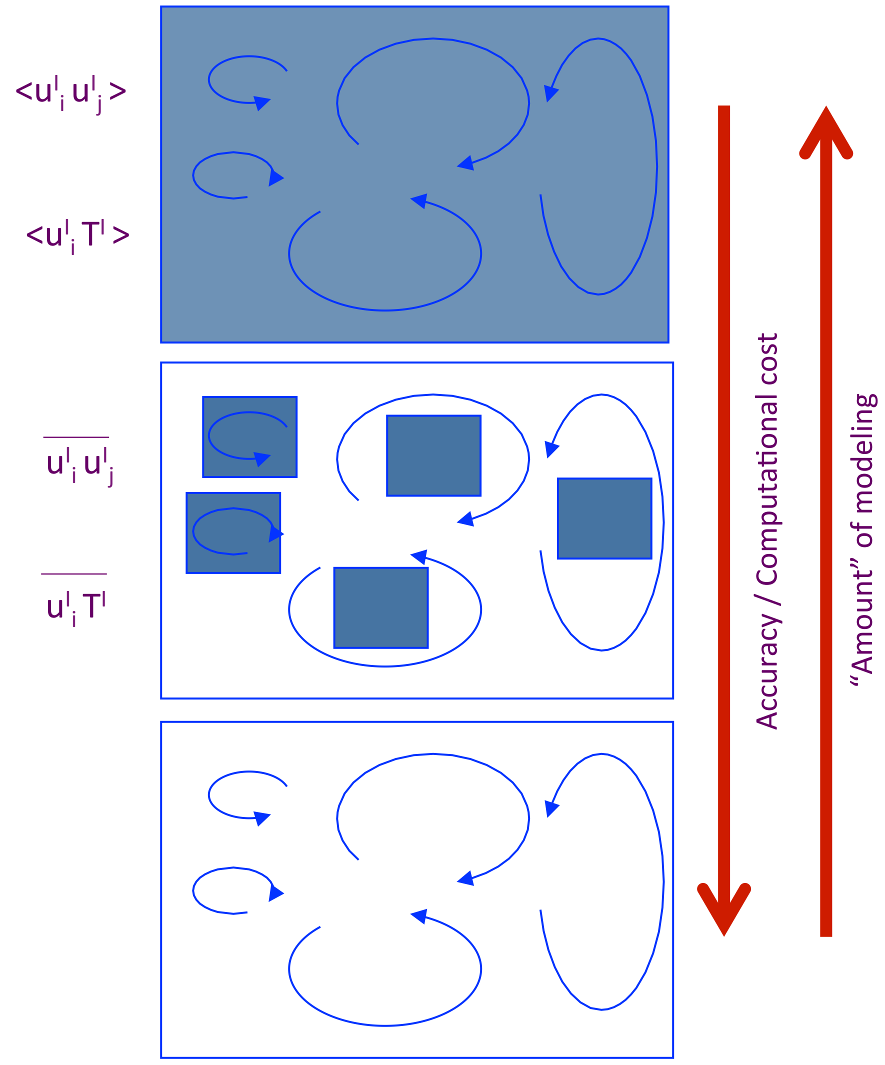

Reynolds Averaged Techniques

- Need extensive empirical data for constants
- Geometry specific
- Underlying assumption of isotropy (sometimes)

Volume Averaging (LES)

- Resolve the large eddies
- Average over small scales
- Simple universal models (maybe)

Direct Numerical Simulation (DNS)

- Valid for resolution finer than smaller eddies
- Applicabile to low Reynolds number turbulent flows (computational cost limitations)

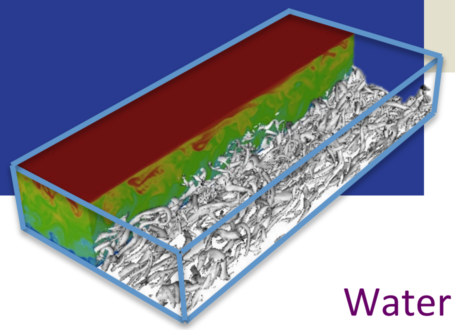

Multiphase Flow Laboratory
University of Udine

Eddy size and frequencies: A "dimensional" example

Water flowing through a pipe with 50 mm diameter at velocity 1.8 m/s.

$$Re \approx 10^5$$

"Type" of Eddy:	Size	Frequency
Largest Eddies	25 mm	3.5 Hz
Energy Containing Eddies	0.6 mm	140 Hz
Most Dissipative Eddies	0.125 mm=125µm	450 Hz
Kolmogorov Eddies	0.025 mm=25µm	1300 Hz

Computational cost for a DNS:

$$\left(\frac{L}{\eta_K}\right)^3 \left(\frac{T}{\tau_K}\right) \propto \mathrm{Re}^{3.6} \left\{ \begin{array}{l} N_x \times N_y \times N_z \propto \mathrm{Re}^{2.7} \\ N_t \propto \mathrm{Re}^{0.9} \end{array} \right.$$

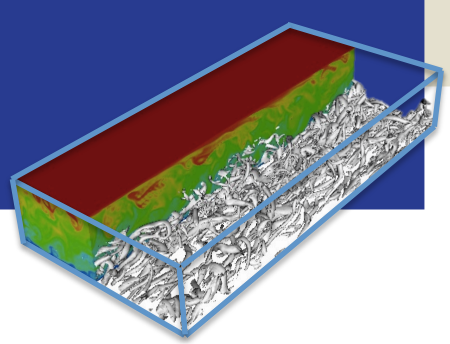

Compare computational costs: DNS vs LES

Grid resolution requirements for LES of turbulent boundary layers

(see Piomelli, *Philos Trans A Math Phys Eng Sci*, vol. 372, 2014):

"Type" of LES	Spatial resolution
Resolve outer layer eddies (domain L_x x L_y x d)	$\propto Re^{0.4}$
Resolve inner layer eddies (wall-resolved LES)	$\propto Re^{1.8}$
LES with wall models	$\propto Re$

with δ = boundary layer thickness (separates inner and outer layer)

Total computational cost for a LES: up to $Re^{2.4}$

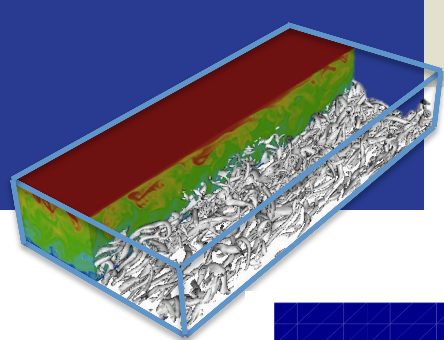

Lagrangian description of particles

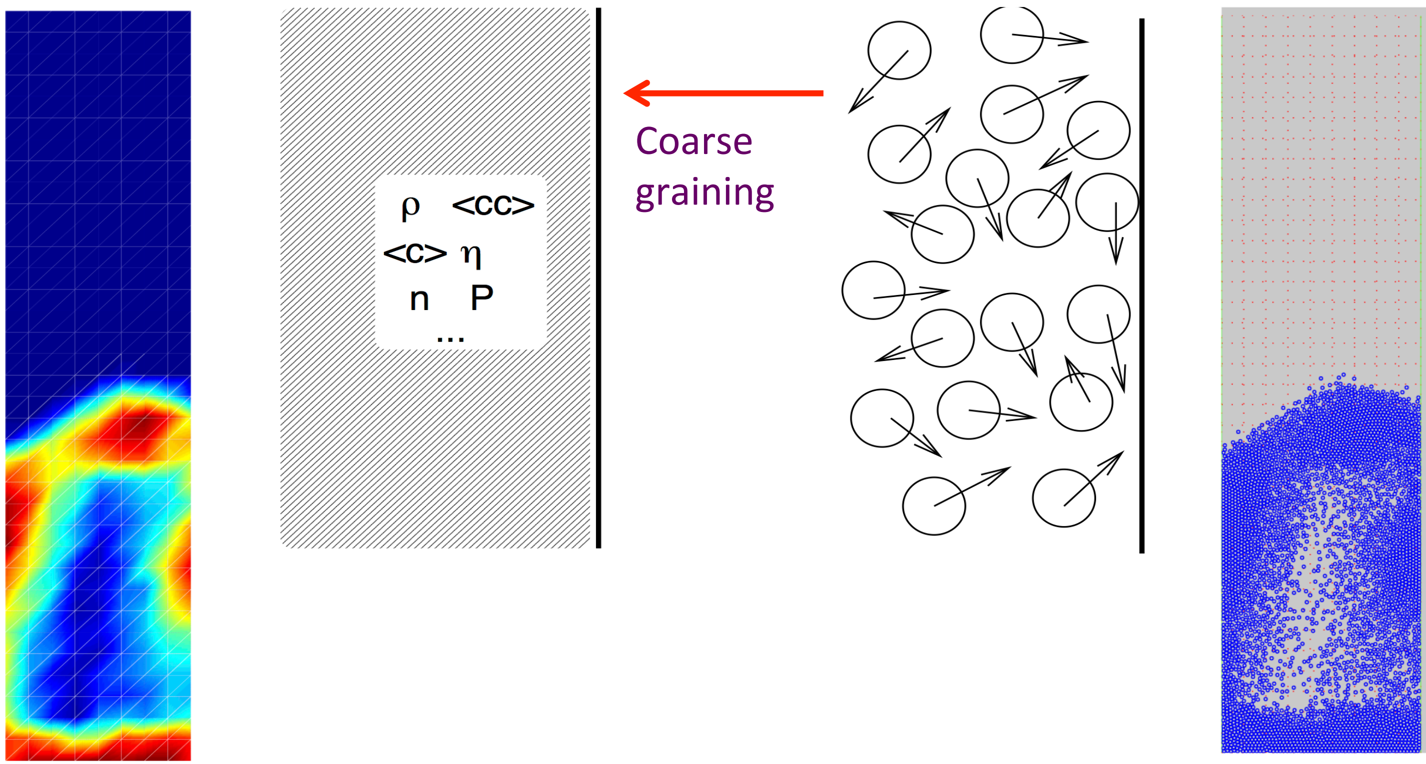

Eulerian Approach: use separate Eulerian balance equations for both phases (treated as two inter-penetrating continua), coupled through inter-phase exchange terms.

Lagrangian Approach: the trajectory of each particle and subsequent averaging (over all tracked particles) is simulated explicitly.

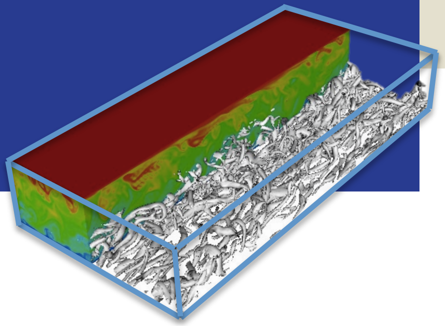

Lagrange tracking of pointwise particles

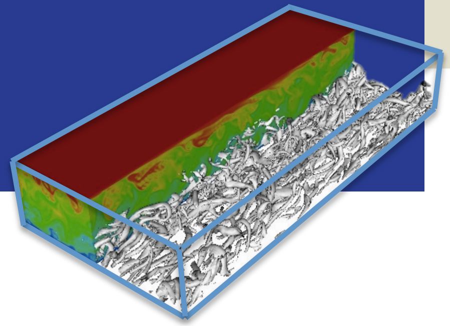

Forces Acting on a Particle

Drag

Gravity & Buoyancy

$$\frac{d\, m_p\, \mathbf{v}_p}{d\, t} = -\, 3\,\pi\, d_p\, \mu\, (\mathbf{v}_p - \mathbf{v}) \;+\; (m_p - m_f)\,\mathbf{g}$$

$$+\; m_f \frac{D\mathbf{v}}{D\, t} \;-\; \frac{1}{2}\, m_f \left(\frac{d\mathbf{v}_p}{d\, t} - \frac{D\mathbf{v}}{D\, t} \right)$$

$$-\; \frac{3}{2}\,\pi\, {d_p}^2\, \mu \int_0^t \left(\frac{d\mathbf{v}_p}{d\tau} - \frac{d\mathbf{v}}{d\tau} \right) \frac{d\tau}{[\pi\,\nu\,(t-\tau)]^{0.5}}$$

$$\left[\; +\; m_f\, C_L\, (\mathbf{v} - \mathbf{v}_p) \times \boldsymbol{\omega} \;\right]$$

Particle Inertia

Added Mass

Pressure Gradient

Lift

Basset (history)

See: Poisson (1831); Stokes (1845); Basset (1888); Oseen (1911); Faxen (1922); Gatignol (1983); Maxey & Riley (1983)

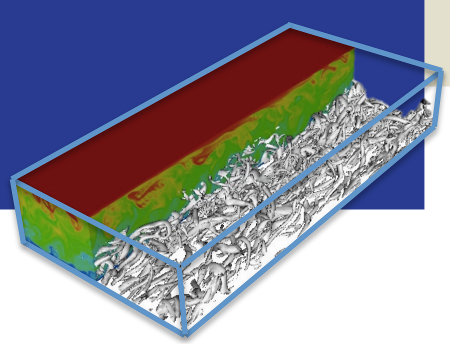

Forces Acting on a Particle

$$F_{drag} \rightarrow O\left(St^{-1}\right)$$

$$F_{prgr} \rightarrow O\left(\frac{\rho_f}{\rho_p}\right)$$

$$F_{addm} \rightarrow O\left(\frac{\rho_f}{\rho_p}\right)$$

$$F_{Bass} \rightarrow O\left(\left(\frac{\rho_f}{\rho_p}\right)^{1/2}\right)$$

$$F_{lift} \rightarrow O\left(d_p{}^2 \frac{\sqrt{dv\ /\ dy}}{\nu}\right)$$

Good news:

for small heavy particles only drag and gravity matter!!

Effect of other forces on particle motion is negligible.

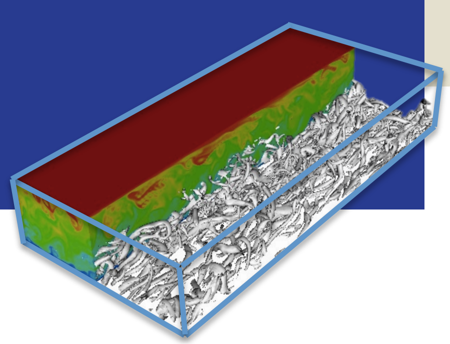

Minimal "Stokesian" model for Lagrangian Particle Tracking

In the limit of small (pointwise) heavy particles:

$$\boxed{\frac{d\mathbf{v}_p}{dt} = \frac{\mathbf{v}-\mathbf{v}_p}{\tau_p \cdot f(\mathrm{Re}_p)} - \mathbf{g}\left(1-\frac{\rho_f}{\rho_p}\right)}$$

Controlling parameters: τ_p and Re_p

Particle Timescale: $\tau_p = d_p^2\, \rho_p / 18\, \mu$

Flow Timescale: $\tau_f = L/U = \nu / u_\tau^2$

Particle Stokes number: $St = \tau_p / \tau_f$

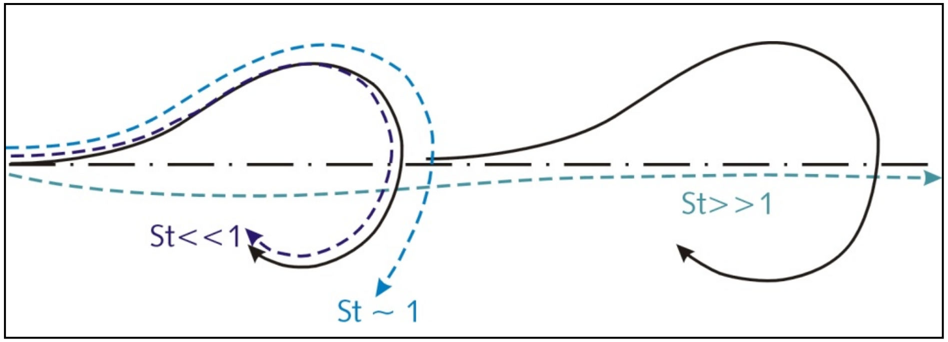

Recall: in such minimal model, inertia controls particle dynamics and particle-turbulence interactions

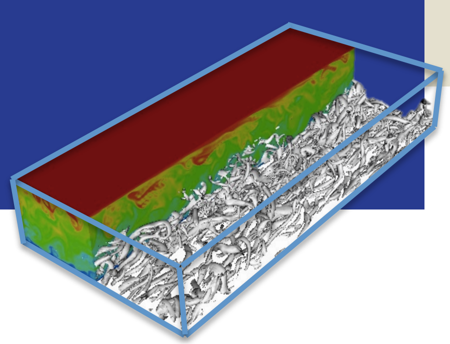

Flow anisotropy effects on fluid flow time scales

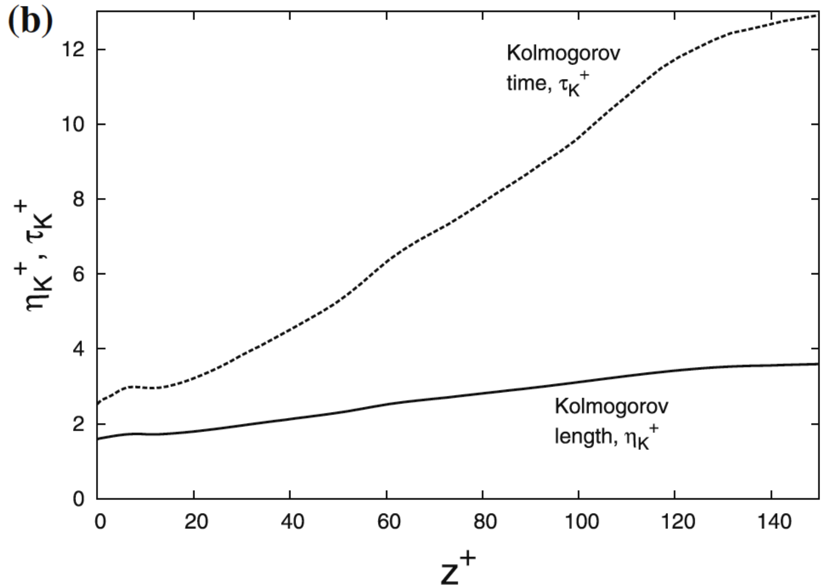

Kolmogorov time/length:

$\tau_K^+ = \tau_K / \tau_f$

$\eta_K^+ = \eta_K / \eta_f$

Renormalized Stokes number:

$St_K = \tau_p / \tau_K$

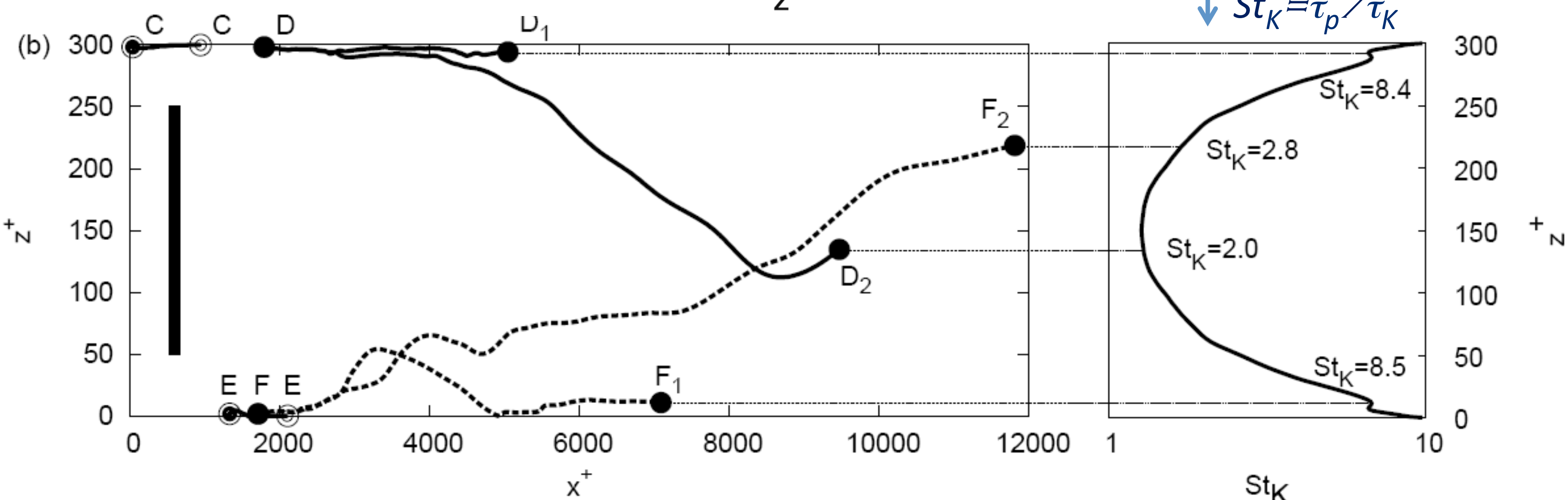

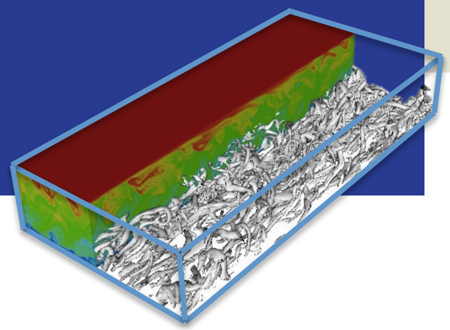

Lagrange tracking of non-spherical pointwise particles

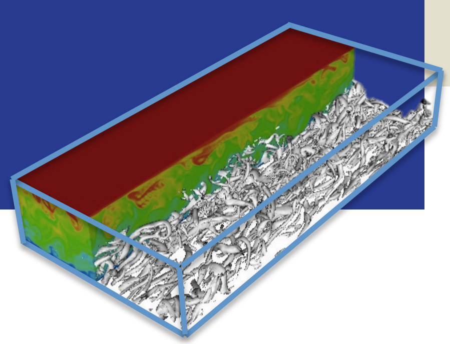

Modelling non-spherical particles as pointwise particles

Consider (again!) the simplest dynamical model (point-particles in creeping flow) for the simplest non-spherical shape (rod/ellipsoid):

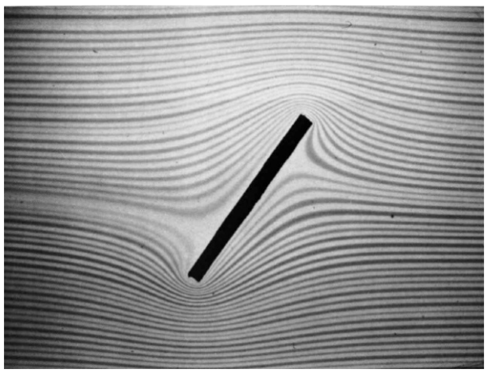

No wake -> Stokes flow

$$\boxed{\mathrm{Re}_p = \frac{u_{rel} L}{\nu} << 1}$$

$\lambda = L / D$ Aspect ratio

θ Orientation

L , D << η_K , Δ -> Pointwise

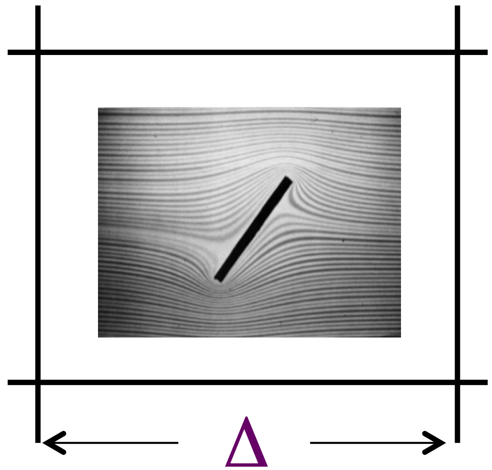

$$\boxed{m_p \frac{d\mathbf{v}_p}{dt} = \sum_i \mathbf{F}_i}$$

Force model

Drag <- Fluid action
+
Particle orientation

$$\boxed{C_D = \frac{\mathbf{F}_D}{\frac{1}{2}\rho \mathbf{u}_{rel}^2 A_p} = f(\mathrm{Re}_p, \lambda, \theta)}$$

The pointwise approximation for non-spherical particles

The simplest approach to deal with non-spherical particles is to describe their translation and rotation with a "lumped-variable" model

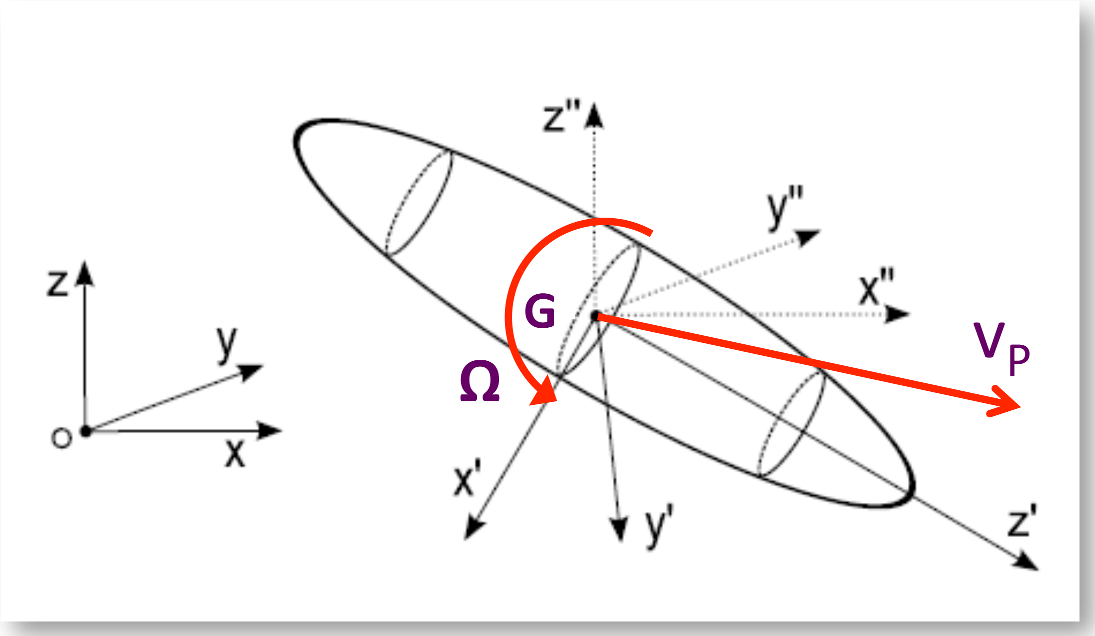

Basically, particle = Lagrangian point moving in 3D space. Finite-size effects neglected!

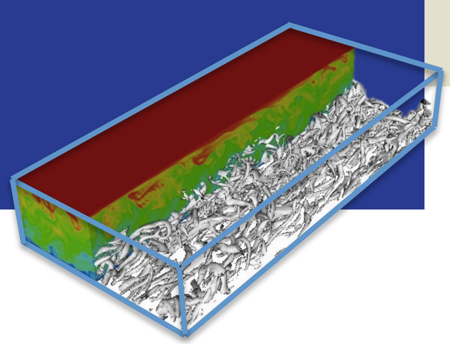

Lagrangian equations of motion for non-spherical particles

- Translational dynamics (enough for a spherical particle)

$$m_p \frac{d\mathbf{v}_p}{dt} = \sum_i \mathbf{F}_i = \mathbf{F}_D + \mathbf{F}_g + \mathbf{F}_L + \mathbf{F}_{PG} + \mathbf{F}_{AM} + \mathbf{F}_B + \ldots$$

- Rotational dynamics (needed for a non-spherical particle)

$$\begin{cases} I_x \dfrac{d\omega_x}{dt} = \sum_i T_{x,i} + \omega_y \omega_z \left(I_y - I_z\right) \\ I_y \dfrac{d\omega_y}{dt} = \sum_i T_{y,i} + \omega_z \omega_x \left(I_z - I_x\right) \\ I_z \dfrac{d\omega_z}{dt} = \sum_i T_{z,i} + \omega_x \omega_y \left(I_x - I_y\right) \end{cases}$$

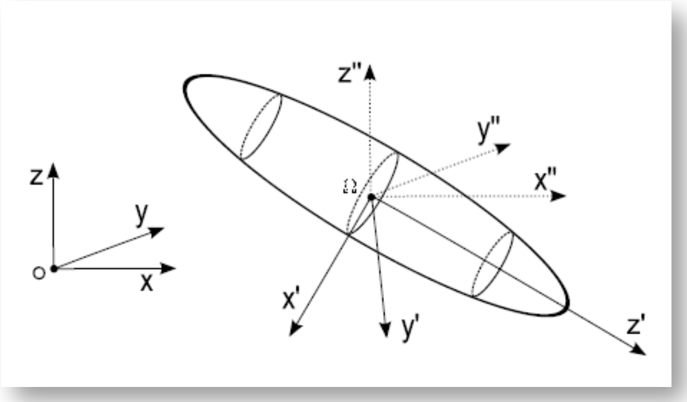

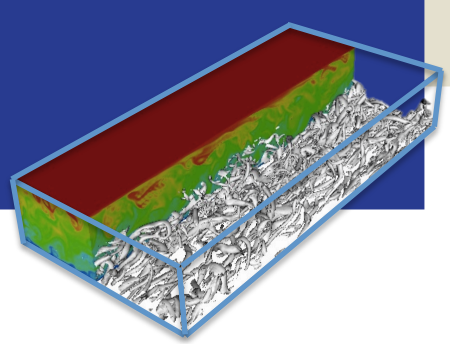

Modelling forces for non-spherical particles

Consider translational dynamics first.

We need force models that account for shape and orientation.

One option is to assume **creeping flow** conditions.

For drag:
(Oberbeck, 1876)

$$\boxed{f_\lambda = \frac{F_D\left(\lambda, Re_p \to 0\right)}{3\pi d_p \mu_f u_{rel}}}$$

$$\boxed{f_{\lambda\|} = \frac{(4/3)\lambda^{-1/3}(1-\lambda^2)}{\lambda - \dfrac{(2\lambda^2-1)\ln\left(\lambda+\sqrt{\lambda^2-1}\right)}{\sqrt{\lambda^2-1}}}}$$

$$\boxed{f_{\lambda\perp} = \frac{(8/3)\lambda^{-1/3}(\lambda^2-1)}{\lambda + \dfrac{(2\lambda^2-3)\ln\left(\lambda+\sqrt{\lambda^2-1}\right)}{\sqrt{\lambda^2-1}}}}$$

$$\boxed{\mathbf{F}_D\left(\lambda, Re_p \to 0\right) = 3\pi d_p \mu_f \left(\mathbf{u}_{rel\|} \cdot f_{\lambda\|} + \mathbf{u}_{rel\perp} \cdot f_{\lambda\perp}\right)}$$

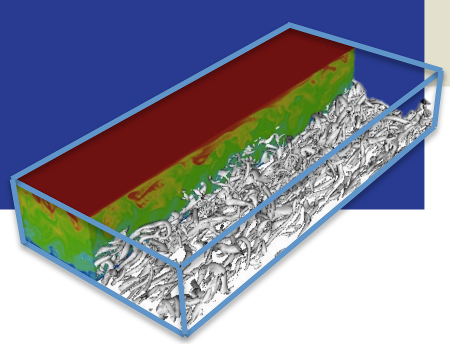

Modelling forces for non-spherical particles

For an ellipsoid:

$$\boxed{\mathbf{F}_D\left(\lambda, \mathrm{Re}_p \to 0\right) = 3\pi d_p \mu_f \left(\mathbf{u}_{rel,1} \cdot f_{\lambda 1} + \mathbf{u}_{rel,2} \cdot f_{\lambda 2} + \mathbf{u}_{rel,3} \cdot f_{\lambda 3}\right)}$$

For a spheroid: $f_{\lambda 1} = f_{\lambda \|}$ and $f_{\lambda 2} = f_{\lambda 3} = f_{\lambda \perp}$

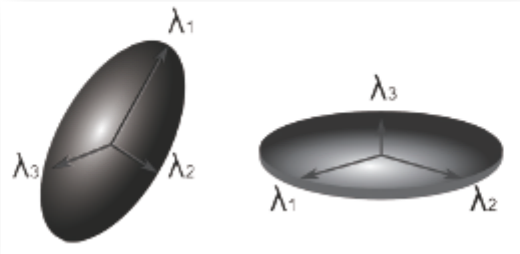

Note 1 - minimum drag shape is obtained:

- for a sphere averaging over all orientations
- for a prolate spheroid with λ=1.955 for stationary orientation (// to symmetry axis)

Note 2 – creeping flow conditions hold if:

$$\boxed{\mathbf{u}_{rel,1} = \mathbf{u}_{f@p} - \mathbf{v}_p \cong 0}$$

(small slip velocity)

and/or if:

$$\boxed{d_p << \eta_f}$$

(small particles, yet not Brownian)

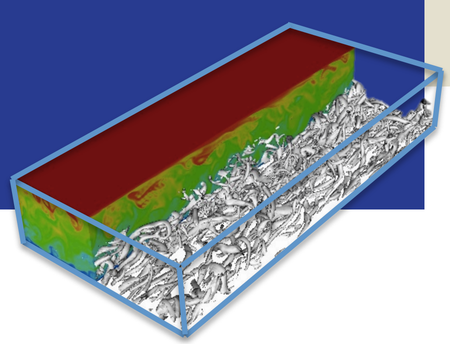

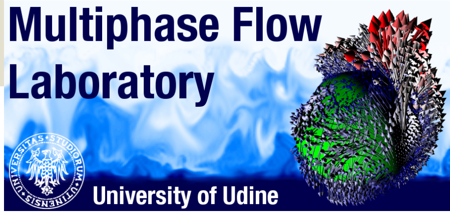

Modelling forces for non-spherical particles

Following Bretherton (1962), Brenner (1964, 1965, 1972), Gallily & Cohen (1979):

$$\boxed{\mathbf{F}_D\left(\lambda, \mathrm{Re}_p \rightarrow 0\right) = 6\pi a \mu_f \overline{\overline{\mathbf{K}}} \cdot \left(\mathbf{u}_{f@p} - \mathbf{v}_p\right)}$$

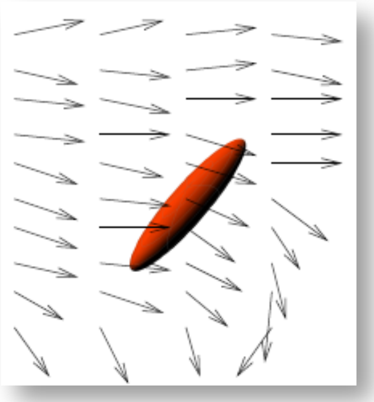

with $\overline{\overline{\mathbf{K}}}$ = translational resistance tensor for arbitrary-shape particle in arbitrary flow field

By analogy, the shear-induced lift force model is:

$$\boxed{C_L = \frac{\mathbf{F}_L(\mathrm{Re}_p \rightarrow 0, \lambda)}{\frac{1}{2}\rho \mathbf{u}_{rel}^2 \frac{\pi}{4} d_p^2}} \rightarrow \boxed{\mathbf{F}_L\left(\lambda, \mathrm{Re}_p \rightarrow 0\right) = \frac{\pi^2 \mu_f a^2}{\sqrt{\nu}} \Gamma \cdot \overline{\overline{\mathbf{L}}} \cdot \left(\mathbf{u}_{f@p} - \mathbf{v}_p\right)}$$

with:

$$\boxed{\Gamma = \left({\partial u_{f@p,i}} / {\partial x_j} \right) \cdot \left(\left| {\partial u_{f@p,i}} / {\partial x_j} \right| \right)^{-1/2}}$$

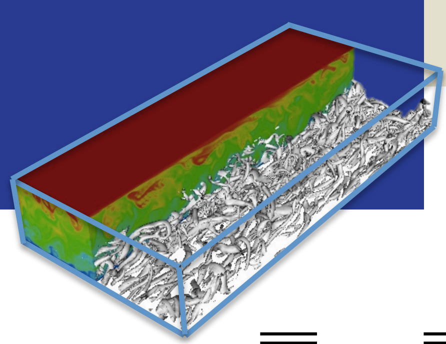

Modelling forces for non-spherical particles

Tensors $\overline{\overline{\mathbf{K}}}$ and $\overline{\overline{\mathbf{L}}}$ can be conveniently expressed wrt a frame of reference with:

- origin at the particle center of mass
- axes being the principal axes of the particle

The "usual" approach is to consider:

1. Inertial Frame X=[x,y,z]

2. Particle Frame X'=[x',y',z']

3. Co-moving frame X"=[x",y",z"]

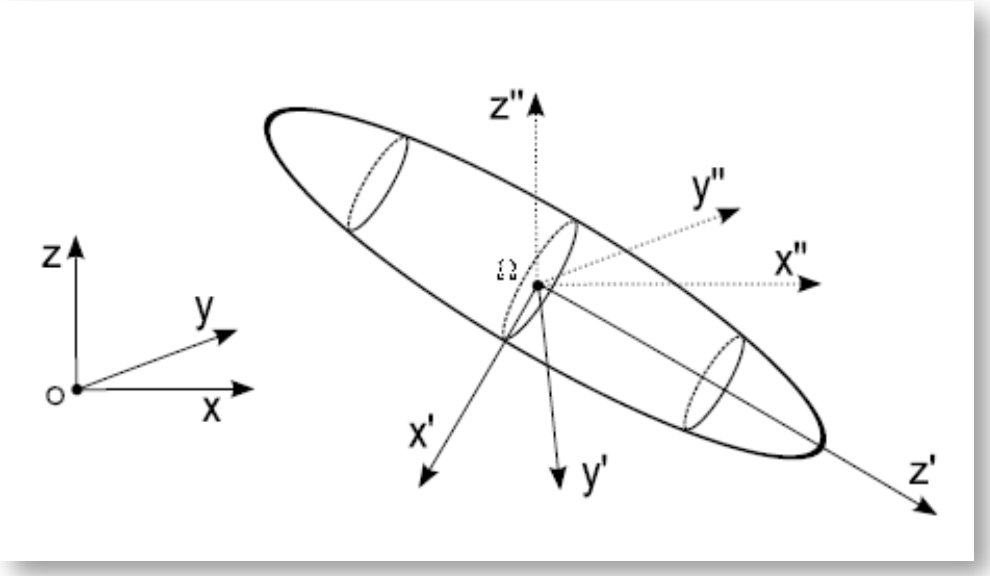

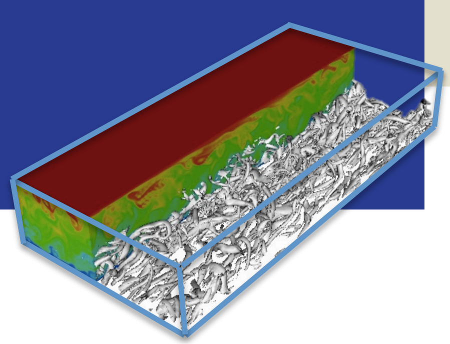

Modelling forces for non-spherical particles

Multiphase Flow Laboratory
University of Udine

In the particle frame:

$$\overline{\overline{\mathbf{K}}}' = \begin{bmatrix} k_{x'x'} & 0 & 0 \\ 0 & k_{y'y'} & 0 \\ 0 & 0 & k_{z'z'} \end{bmatrix}$$

For prolate particles:

$$k_{x'x'} = k_{y'y'} = \frac{(1-\lambda^2)}{\lambda - \dfrac{(2\lambda^2-1)\ln\left(\lambda+\sqrt{\lambda^2-1}\right)}{\sqrt{\lambda^2-1}}}$$

$$k_{z'z'} = \frac{(\lambda^2-1)}{\lambda + \dfrac{(2\lambda^2-3)\ln\left(\lambda+\sqrt{\lambda^2-1}\right)}{\sqrt{\lambda^2-1}}}$$

See also: Brenner, 1964; Happel & Brenner, 1983

$$\overline{\overline{\mathbf{L}}}' = \begin{bmatrix} 0.0501 & 0.0329 & 0.00 \\ 0.0182 & 0.0173 & 0.00 \\ 0.00 & 0.00 & 0.0373 \end{bmatrix}$$

Note: for a sphere the original Saffman model is recovered

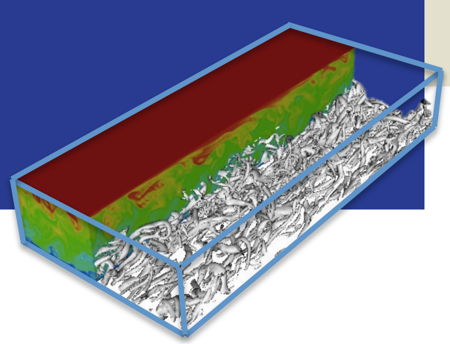

Modelling forces for non-spherical particles

In the particle frame:

$$\overline{\overline{\mathbf{K}}}' = \begin{bmatrix} k_{x'x'} & 0 & 0 \\ 0 & k_{y'y'} & 0 \\ 0 & 0 & k_{z'z'} \end{bmatrix}$$

For oblate particles:

$$K'_{xx} = K'_{yy} = \frac{32\pi a(1-\lambda^2)^{3/2}}{(3-2\lambda^2)(\pi - C) - 2\lambda(1-\lambda^2)^{1/2}}$$

$$K'_{zz} = \frac{16\pi a(1-\lambda^2)^{3/2}}{(1-2\lambda^2)(\pi - C) + 2\lambda(1-\lambda^2)^{1/2}}$$

See also: Brenner, 1964; Happel & Brenner, 1983

$$\overline{\overline{\mathbf{L}}}' = \begin{bmatrix} 0.0501 & 0.0329 & 0.00 \\ 0.0182 & 0.0173 & 0.00 \\ 0.00 & 0.00 & 0.0373 \end{bmatrix}$$

Note: for a sphere the original Saffman model is recovered

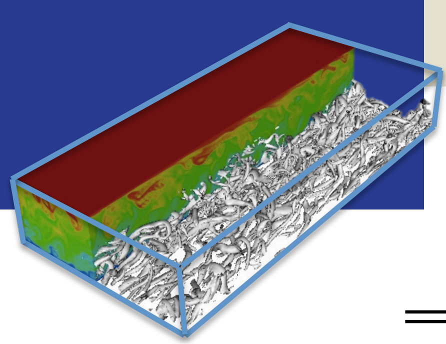

Rigid body kinematics

How to go from $\bar{\bar{\mathbf{K}}}'$ to $\bar{\bar{\mathbf{K}}}$?

$$\boxed{\bar{\bar{\mathbf{K}}}_{(\varphi,\theta,\psi)} = R_{eul}^T \bar{\bar{\mathbf{K}}}' R_{eul}}$$

where R_{Eul} = rotation matrix, obtained from the quaternions:

- $e_0 = \cos\left[\frac{1}{2}(\psi+\varphi)\right]\cos\left(\frac{\theta}{2}\right)$
- $e_1 = \cos\left[\frac{1}{2}(\psi-\varphi)\right]\sin\left(\frac{\theta}{2}\right)$
- $e_2 = \sin\left[\frac{1}{2}(\psi-\varphi)\right]\sin\left(\frac{\theta}{2}\right)$
- $e_3 = \sin\left[\frac{1}{2}(\psi+\varphi)\right]\cos\left(\frac{\theta}{2}\right)$
- $e_0^2 + e_1^2 + e_2^2 + e_3^2 = 1$

$$\begin{pmatrix} \dot{e}_0 \\ \dot{e}_1 \\ \dot{e}_2 \\ \dot{e}_3 \end{pmatrix} = \frac{1}{2}\begin{bmatrix} e_0 & -e_1 & -e_2 & e_3 \\ e_1 & e_0 & -e_3 & e_2 \\ e_2 & e_3 & e_0 & -e_1 \\ e_3 & -e_2 & e_1 & e_0 \end{bmatrix} \cdot \begin{pmatrix} 0 \\ \omega_{x'} \\ \omega_{y'} \\ \omega_{z'} \end{pmatrix}$$

$$R_{eul} = \begin{bmatrix} e_0^2+e_1^2-e_2^2-e_3^2 & 2(e_1e_2+e_0e_3) & 2(e_1e_3-e_0e_2) \\ 2(e_1e_2-e_0e_3) & e_0^2-e_1^2+e_2^2-e_3^2 & 2(e_2e_3+e_0e_1) \\ 2(e_1e_3+e_0e_2) & 2(e_2e_3-e_0e_1) & e_0^2-e_1^2-e_2^2+e_3^2 \end{bmatrix}$$

Note: quaternions prevent gimbal lock problems (matrix singularities) but require normalization at each time step

Rigid body kinematics

In summary, compute the resistance tensor in the particle frame as:

$$\mathbf{F}'_{drag} = \mu \pi a \bar{\bar{\mathbf{K}}}'(\mathbf{u}' - \mathbf{v}')$$

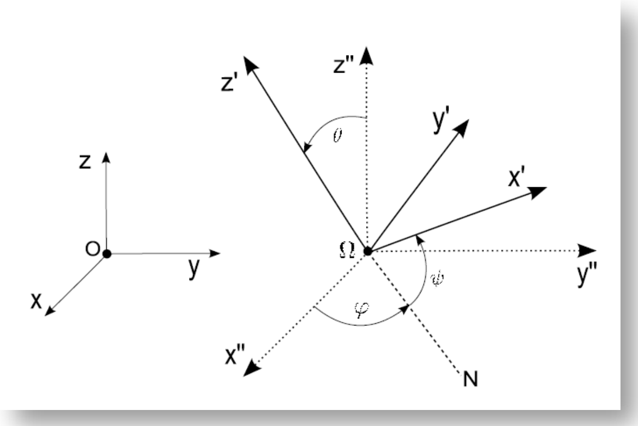

then apply the transformation from the particle frame to the inertial frame:

$$\mathbf{F}_{drag} = R_{eul}^{-1}\mathbf{F}'_{drag} = R_{eul}^{T}\mathbf{F}'_{drag} = \mu \pi a R_{eul}^{T} \bar{\bar{\mathbf{K}}}'(\mathbf{u}' - \mathbf{v}') =$$

$$= \mu \pi a R_{eul}^{T} \bar{\bar{\mathbf{K}}}'(R_{eul}\mathbf{u} - R_{eul}\mathbf{v}) = \mu \pi a R_{eul}^{T} \bar{\bar{\mathbf{K}}}' R_{eul}(\mathbf{u} - \mathbf{v})$$

to get:

$$\mathbf{F}_{drag} = \mu \pi a \bar{\bar{\mathbf{K}}}_{(\varphi,\theta,\psi)}(\mathbf{u} - \mathbf{v})$$

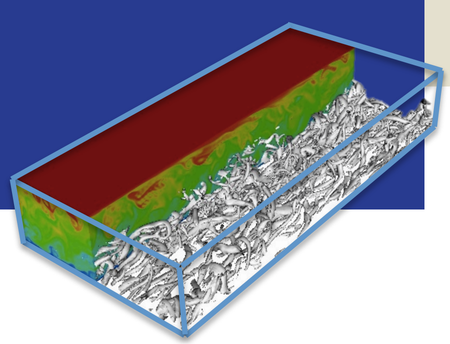

Rigid body kinematics

For the lift force (Harper & Chang, JFM,1968; Hogg , JFM, 1994):

$$\boxed{\mathbf{F}_L = \frac{\pi^2 \mu_f a^2}{\sqrt{\nu}} \Gamma \cdot \left(\overline{\overline{\mathbf{K}}} \cdot \overline{\overline{\mathbf{L}}}' \cdot \overline{\overline{\mathbf{K}}} \right) \cdot \left(\mathbf{u}_{f@p} - \mathbf{v}_p \right)}$$

Note that:

- Lift force is non-zero at any non-zero shear rate
- $\mathbf{F}_L \propto a^2$ with a = semi-minor axis -> lift counts for large particles!
- derived for unidirectional shear
- no wall effects included (only available for spheres)
- So far, very little effort done to lift force models for non-spherical particles

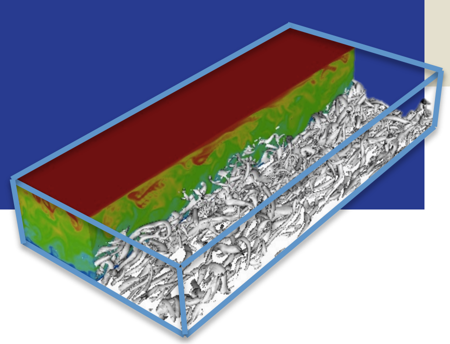

Multiphase Flow Laboratory
University of Udine

"Final" equation of translational motion

$$\overbrace{m_p \frac{d\mathbf{v}_p}{dt}}^{\text{Inertia}} = \overbrace{\mu_f \pi a \overline{\overline{\mathbf{K}}}_{(\varphi,\theta,\psi)} \cdot \left(\mathbf{u}_{f@p} - \mathbf{v}_p\right)}^{\text{Drag}} +$$

$$+ \underbrace{\frac{\pi^2 \mu_f a^2}{\sqrt{\nu}} \Gamma \cdot \left(\overline{\overline{\mathbf{K}}} \cdot \overline{\overline{\mathbf{L}}}' \cdot \overline{\overline{\mathbf{K}}}\right) \cdot \left(\mathbf{u}_{f@p} - \mathbf{v}_p\right)}_{\text{Lift}} + \underbrace{(m_p - m_f)\mathbf{g}}_{\text{Buoyancy}}$$

plus $\dfrac{d\mathbf{x}_p}{dt} = \mathbf{v}_p$ to compute particle trajectory

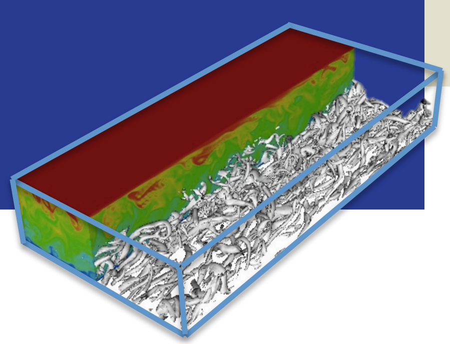

Rotational dynamics

Start from the 2nd cardinal eq. of dynamics in the particle frame:

$$\begin{cases} I_{x'x'}\dot{\omega}_{x'} + \omega_{y'}\omega_{z'}(I_{z'z'} - I_{y'y'}) = M_{x'}^{est} \\ I_{y'y'}\dot{\omega}_{y'} + \omega_{x'}\omega_{z'}(I_{z'z'} - I_{x'x'}) = M_{y'}^{est} \\ I_{z'z'}\dot{\omega}_{z'} + \omega_{x'}\omega_{y'}(I_{y'y'} - I_{x'x'}) = M_{z'}^{est} \end{cases}$$

Note - in the particle frame the inertia tensor is constant:

$$I_{x'x'} = I_{y'y'} = \frac{(1+\lambda^2)a^2}{5} m_P$$

$$I_{z'z'} = \frac{2a^2}{5} m_P \quad .$$

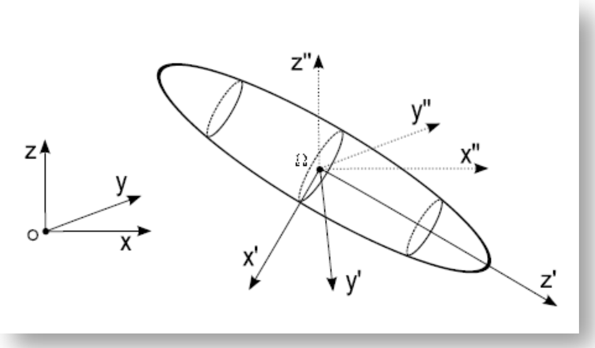

with: $m_p = 4\pi a^3 \lambda \bar{\rho}_p / 3$

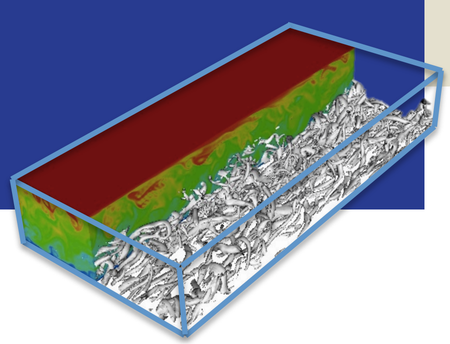

Rotational dynamics

The hydrodynamic torque acting on the particle wrt the principal axes of the particle is computed using Jeffery's formulation (Jeffery, 1922):

$$M_{x'}^{Jeff} = \frac{16\pi\mu a^3\lambda}{3(\beta_0+\lambda^2\gamma_0)}\left[(1-\lambda^2)f' + (1+\lambda^2)(\xi' - \omega_{x'})\right]$$

$$M_{y'}^{Jeff} = \frac{16\pi\mu a^3\lambda}{3(\alpha_0+\lambda^2\gamma_0)}\left[(\lambda^2-1)g' + (1+\lambda^2)(\eta' - \omega_{y'})\right]$$

$$M_{z'}^{Jeff} = \frac{32\pi\mu a^3\lambda}{3(\beta_0+\alpha_0)}(\chi' - \omega_{z'})$$

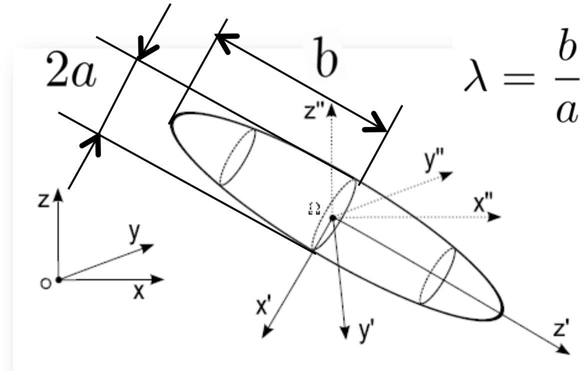

For prolate speroids (Gallily & Cohen, 1979):

$$\alpha_0 = \beta_0 = \frac{2\lambda^2\sqrt{\lambda^2-1} + \lambda \cdot ln\left(\frac{\lambda-\sqrt{\lambda^2-1}}{\lambda+\sqrt{\lambda^2-1}}\right)}{2(\lambda^2-1)^{3/2}}$$

$$\gamma_0 = \frac{2\sqrt{\lambda^2-1} + \lambda \cdot ln\left(\frac{\lambda-\sqrt{\lambda^2-1}}{\lambda+\sqrt{\lambda^2-1}}\right)}{(\lambda^2-1)^{3/2}}$$

For oblate speroids (Sievert et al., 2014):

$$\alpha_0 = \beta_0 = -\frac{\lambda}{2(1-\lambda^2)^{3/2}}[C - \pi + 2\lambda(1-\lambda^2)^{1/2}],$$

$$\gamma_0 = \frac{1}{(1-\lambda^2)^{3/2}}[\lambda C - \lambda\pi + 2(1-\lambda^2)^{1/2}],$$

$$C = 2\tan^{-1}(\lambda(1-\lambda^2)^{-1/2})$$

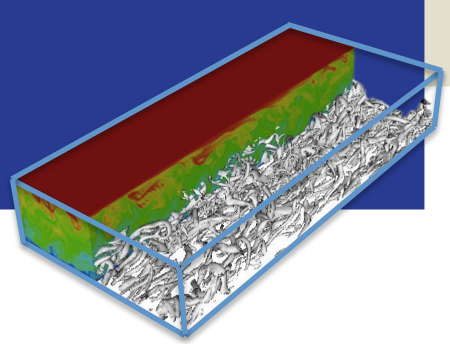

Rotational dynamics

The hydrodynamic torques depend on the elements of:

- rate of strain tensor:

$$S_{ij} = \frac{1}{2}\left(\frac{\partial u_i}{\partial x_j} + \frac{\partial u_j}{\partial x_i}\right)$$

$$f' = \frac{1}{2}\left(\frac{\partial u_{z'}}{\partial y'} + \frac{\partial u_{y'}}{\partial z'}\right)$$

$$g' = \frac{1}{2}\left(\frac{\partial u_{x'}}{\partial z'} + \frac{\partial u_{z'}}{\partial x'}\right)$$

- rate of rotation tensor:

$$\Omega_{ij} = \frac{1}{2}\left(\frac{\partial u_i}{\partial x_j} - \frac{\partial u_j}{\partial x_i}\right)$$

$$\xi' = \frac{1}{2}\left(\frac{\partial u_{z'}}{\partial y'} - \frac{\partial u_{y'}}{\partial z'}\right)$$

$$\eta' = \frac{1}{2}\left(\frac{\partial u_{x'}}{\partial z'} - \frac{\partial u_{z'}}{\partial x'}\right)$$

$$\chi' = \frac{1}{2}\left(\frac{\partial u_{x'}}{\partial y'} - \frac{\partial u_{y'}}{\partial x'}\right)$$

computed in the particle frame: $\bar{\bar{\mathbf{G}}}' = R_{eul}\,\bar{\bar{\mathbf{G}}}\,R_{eul}^T$

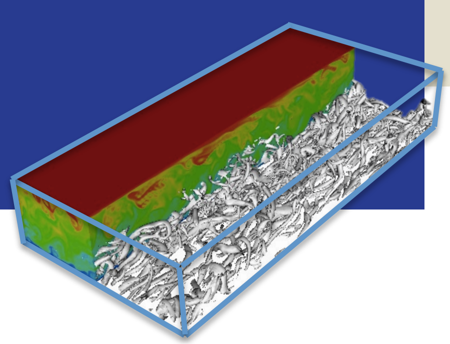

Rotational dynamics

Caveat: How accurate is Jeffery's formulation?

Channel center…

Near the wall…

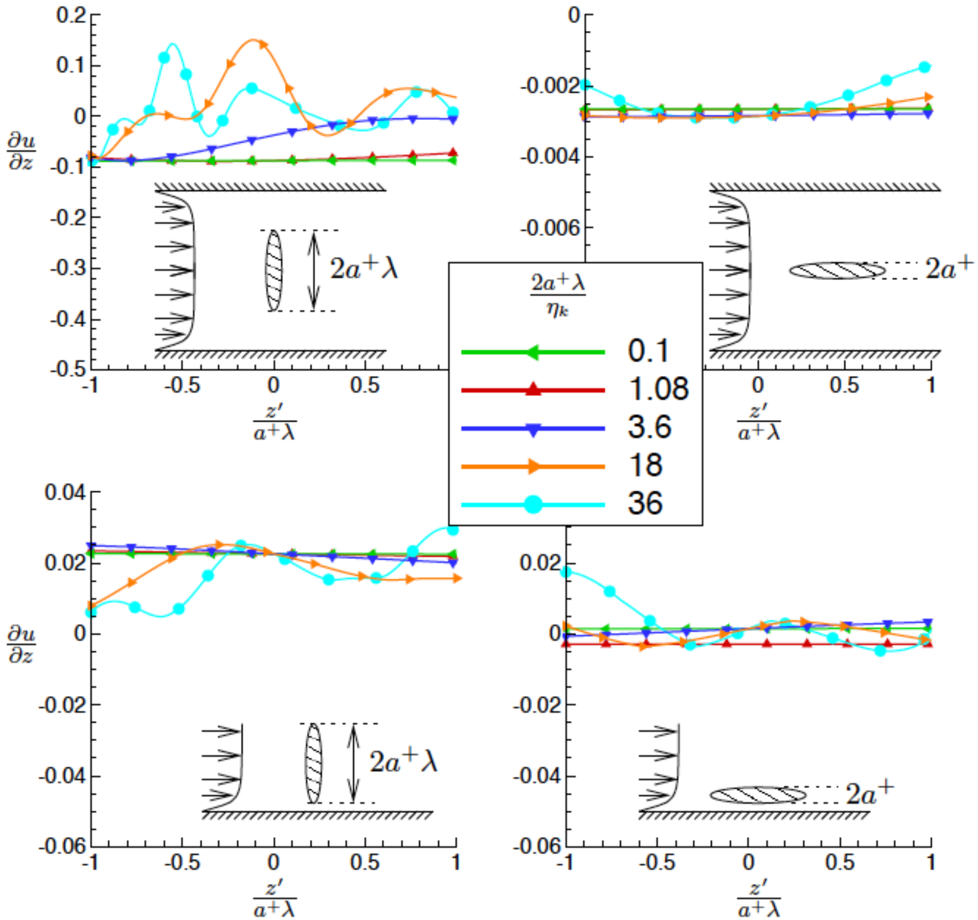

Instantaneous velocity gradient along the ellipsoid at varying aspect ratio

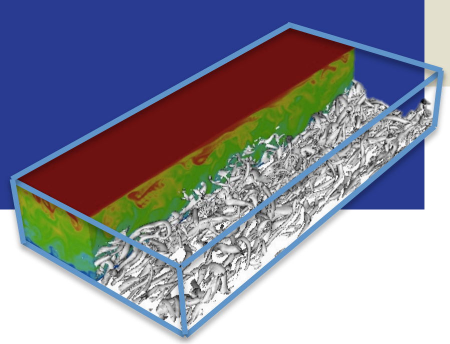

Rotational dynamics

Caveat: How accurate is Jeffery's formulation?

Relative RMS norm:

$$\left\| \overrightarrow{M}_J^a - \overrightarrow{M}_J^c \right\| = \sqrt{\frac{\sum_i \left(\overrightarrow{M}_{J,i}^a - \overrightarrow{M}_{J,i}^c \right)^2}{\sum_i \left(\overrightarrow{M}_{J,i}^c \right)^2}}$$

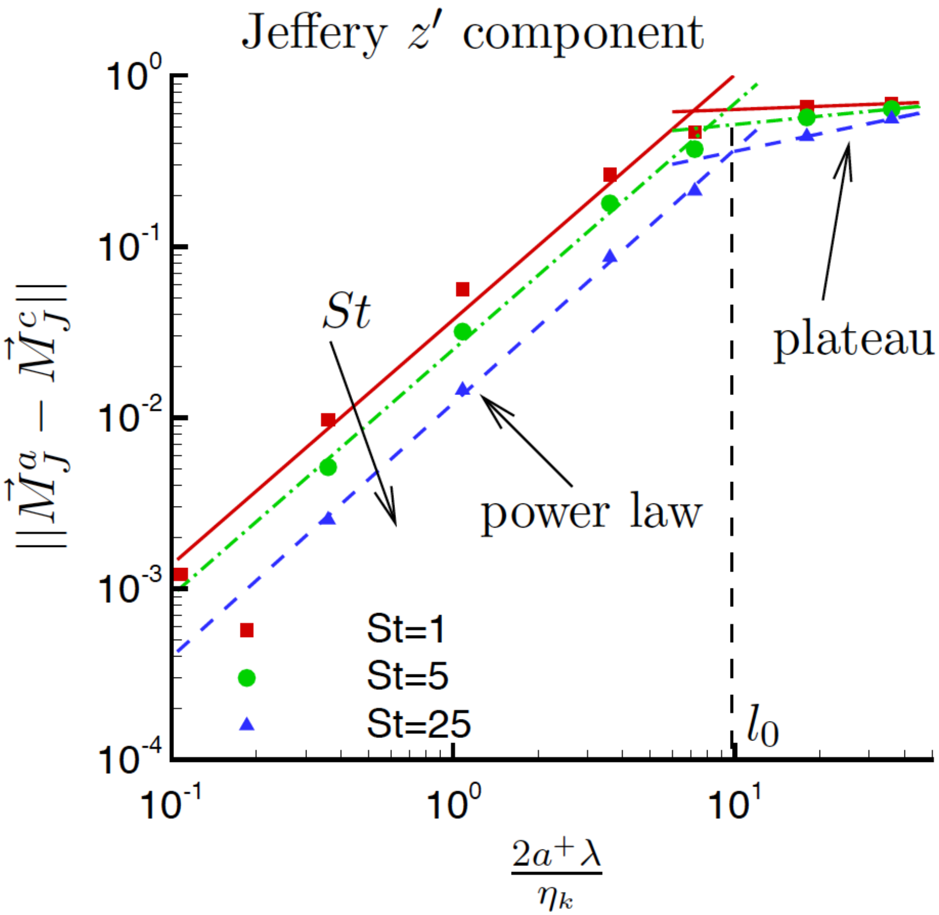

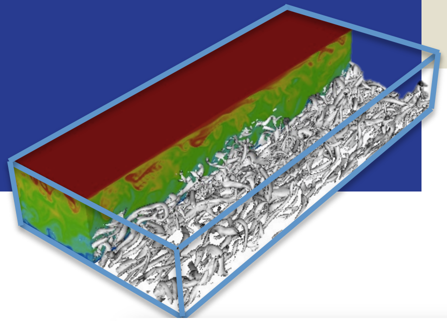

Complete system of equations and controlling parameters

$$
\begin{cases}
\underline{Kinematics:} \\
\dfrac{d\mathbf{x}_{(G)}}{dt} = \mathbf{v} \\
\dot{e_0} = \dfrac{1}{2}(-e_1\omega_{x'} - e_2\omega_{y'} - e_3\omega_{z'}) \\
\dot{e_1} = \dfrac{1}{2}(e_0\omega_{x'} - e_3\omega_{y'} + e_2\omega_{z'}) \\
\dot{e_2} = \dfrac{1}{2}(e_3\omega_{x'} + e_0\omega_{y'} - e_1\omega_{z'}) \\
\dot{e_3} = \dfrac{1}{2}(-e_2\omega_{x'} + e_1\omega_{y'} + e_0\omega_{z'}) \\
\underline{Dynamics:} \\
m_P \dfrac{d\mathbf{v}}{dt} = (m_P - m_F)\mathbf{g} + \mu \bar{\bar{\mathbf{K}}}_{(e_0,e_1,e_2,e_3)} \cdot (\mathbf{u} - \mathbf{v}) \\
I_{x'x'}\dot{\omega}_{x'} + \omega_{y'}\omega_{z'}(I_{z'z'} - I_{y'y'}) = M_{x'}^{Jeff} \\
I_{y'y'}\dot{\omega}_{y'} + \omega_{x'}\omega_{z'}(I_{z'z'} - I_{x'x'}) = M_{y'}^{Jeff} \\
I_{z'z'}\dot{\omega}_{z'} + \omega_{x'}\omega_{y'}(I_{y'y'} - I_{x'x'}) = M_{z'}^{Jeff}
\end{cases}
$$

Aspect ratio (shape) $\lambda = \dfrac{b}{a}$

Specific density $S = \dfrac{\rho_P}{\rho_F}$

Response time (inertia) $St = \dfrac{\tau_P}{\tau_F}$

It can be anticipated that, in such model, particle behaviour is fully characterized by:

1. Stokes number (incorporates all inertial effects)

2. Aspect ratio (incorporates all shape effects)

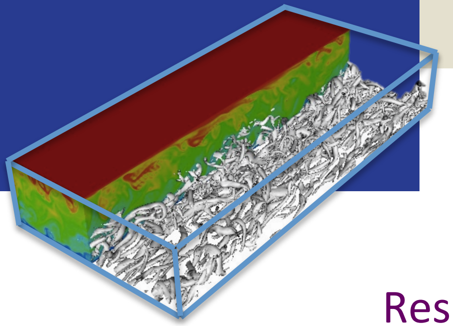

Definition of response time for non-spherical particles

Response time for non-spherical particles: how to define it?

For spheres: $\mathrm{St} = \frac{2}{9} \mathrm{S} \left(a^{+}\right)^{2}$

For ellipsoids:

- Shapiro & Goldenberg (1993) assumed isotropic particle orientation and used the averaged mobility dyadic (inverse of the translation dyadic)

$$\boxed{\mathrm{St} = \frac{4\lambda \mathrm{S} a^{+^2}}{9}\left(\frac{1}{k_{x'x'}} + \frac{1}{k_{y'y'}} + \frac{1}{k_{z'z'}}\right) = \frac{2\lambda \mathrm{S} a^{+^2}}{9} \frac{\ln\left(\lambda + \sqrt{\lambda^2 - 1}\right)}{\sqrt{\lambda^2 - 1}}}$$

- Fan & Ahmadi (1995) used the orientation-averaged translation dyadic

$$\boxed{\mathrm{St} = \frac{4\lambda \mathrm{S} a^{+^2}}{(k_{x'x'} + k_{y'y'} + k_{z'z'})}}$$

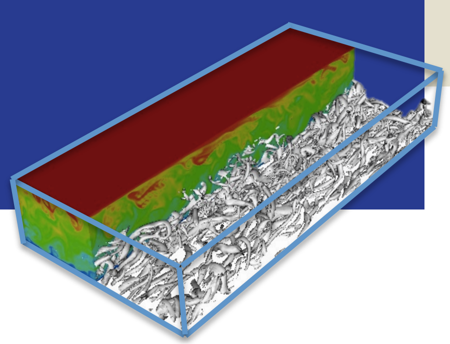

Definition of response time for non-spherical particles

For non-spherical particles also the **rotational response time** is important:

For spheres: $\mathrm{St_r} = \frac{1}{15} \mathrm{S} \left(a^+\right)^2 = \frac{3}{10} \mathrm{St}$

For ellipsoids no widely-used definition provided so far.
No "unique" expression based on isotropy can be obtained.

- rotation around *z′* in the fiber frame:

$$\frac{\mathrm{d}\omega^+_{z'}}{\mathrm{d}t^+} = \frac{20}{(\alpha_0 + \beta_0) S a^{+2}} \Delta\omega^+_{z'} = \frac{1}{\tau^+_{r,z'}} \Delta\omega^+_{z'} \rightarrow \boxed{\tau^+_{r,z'} = \frac{\alpha_0 S a^{+2}}{10}}$$

- rotation around *x′* or *y′* in the fiber frame:

$$\frac{\mathrm{d}\omega^+_{y'}}{\mathrm{d}t^+} = \underbrace{\omega^+_{x'}\omega^+_{z'} \left(\frac{2}{1+\lambda^2} - 1\right)}_{A} + \underbrace{\frac{20(\lambda^2 - 1)}{(\alpha_0 + \lambda^2\gamma_0)(1+\lambda^2) S a^{+2}} g'}_{B} + \underbrace{\frac{20(\lambda^2 + 1)}{(\alpha_0 + \lambda^2\gamma_0)(1+\lambda^2) S a^{+2}}}_{1/\tau_{r,y'}} \Delta\omega^+_{y'}$$

$$\rightarrow \boxed{\tau_{r,y'} = \frac{(\alpha_0 + \lambda^2\gamma_0)}{20} S a^{+2} \equiv \tau_{r,x'}}$$

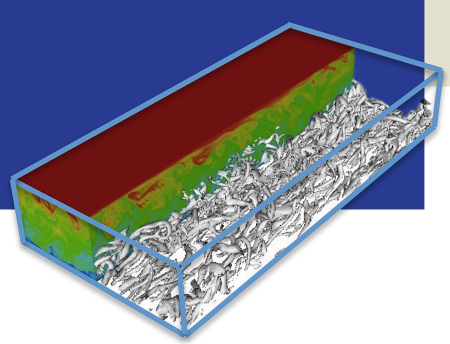

Definition of response time for non-spherical particles

$$\boxed{\tau_{r,y'} = \frac{(\alpha_0+\lambda^2\gamma_0)}{20} Sa^{+2} \equiv \tau_{r,x'}}$$

$$\boxed{\tau^+_{r,z'} = \frac{\alpha_0 Sa^{+2}}{10}}$$

Assume isotropic orientation:

$$\tau_r^+ = \frac{1}{3}(\tau_{r,x'}+\tau_{r,y'}+\tau_{r,z'}) = \frac{2\alpha_0+\lambda^2\gamma_0}{30}Sa^{+2} = \frac{3}{10}\tau_p^+ \quad \forall\lambda$$

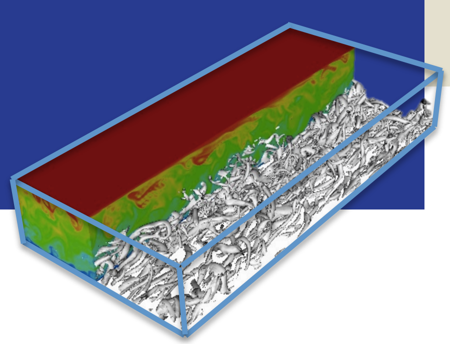

Example of collective behaviour

Rigid fibers in TCF

$\mathbf{x}(t,\lambda)$, $\mathbf{v}(\mathbf{x}(t,\lambda),t,\lambda)$, $\omega(\mathbf{x}(t,\lambda),t,\lambda)$

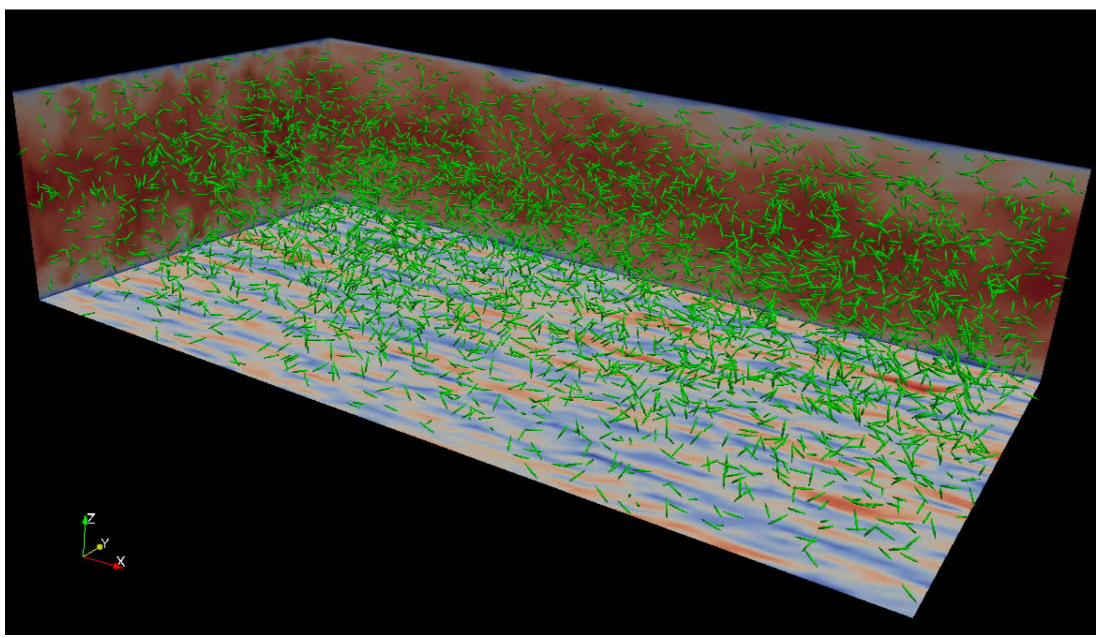

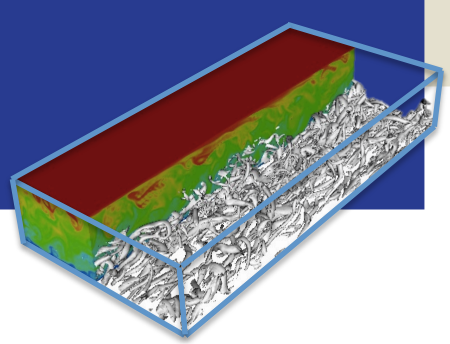

Rigid fibers in TCF

Sources of bias: Inertia + Elongation

Dilute suspension of small rigid fibers in a turbulent channel (Re_τ=300)

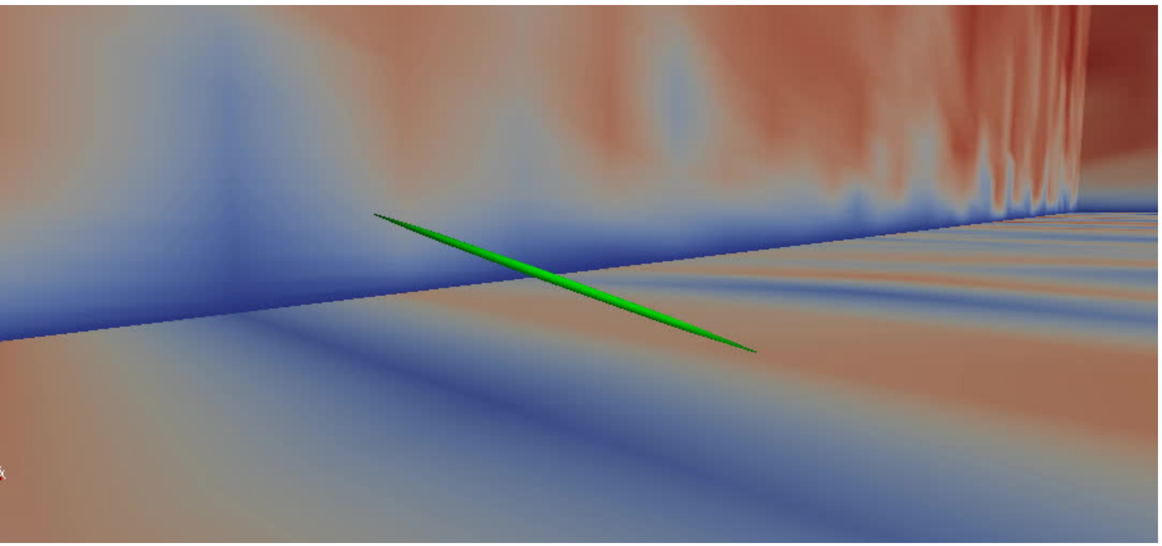

Particle functionality added in the model: **Elongation**

$$\frac{d\mathbf{x}_p}{dt} = \mathbf{v}_p, \quad m_p \frac{d\mathbf{v}_p}{dt} = \sum_i \mathbf{F}_i$$

$$\frac{d(\mathbf{I}\omega_p)}{dt} = \sum_i \mathbf{T}_i$$

$$\mathbf{F}_D = \mu \mathbf{A}^t \mathbf{K}' \mathbf{A} \cdot (\mathbf{u}_f - \mathbf{u}_p)$$

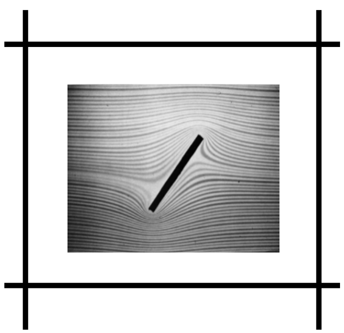

Assumptions:

- fibers = non-interacting ellipsoids with uniform mass distribution in dilute flow
- fiber size < Kolmogorov length scale
- ignore lubrication forces, aggregation/breakage

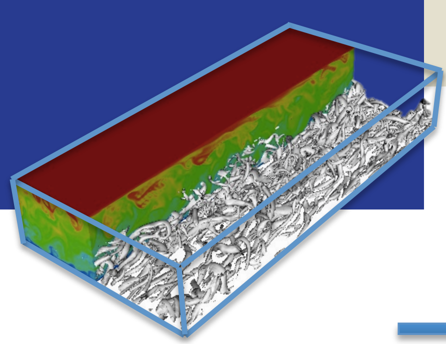

Rigid fibers in TCF

Sources of bias: Inertia + Elongation

Fiber parameters in the animations: St = 30, λ = 50, a^+ = 0.36

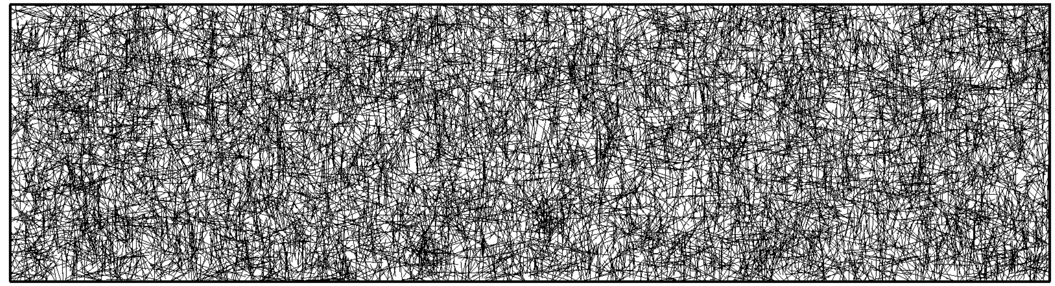

Front view

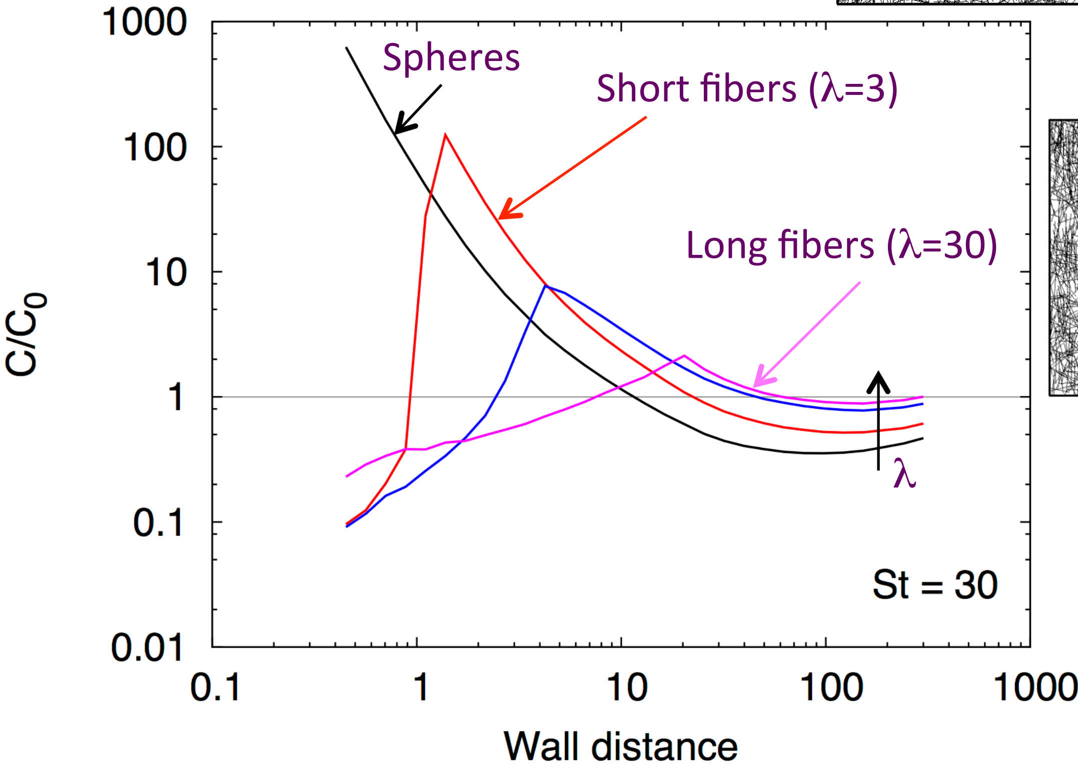

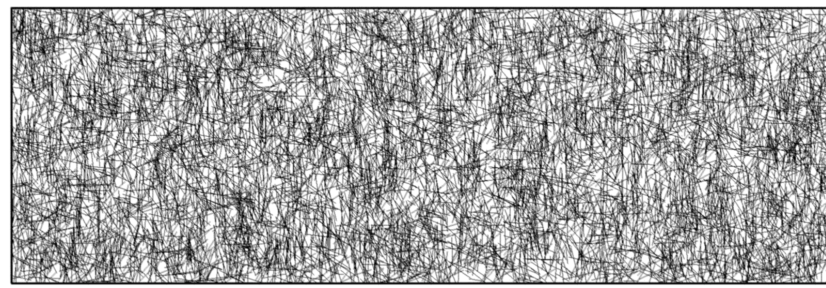

Side view

Effect of fiber elongation on near-wall accumulation

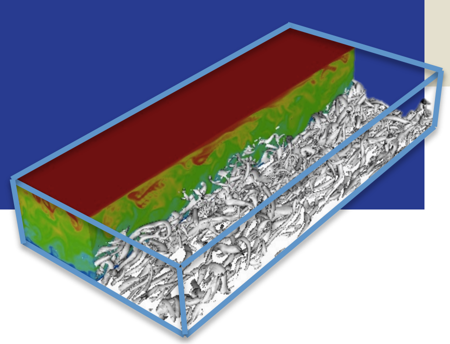

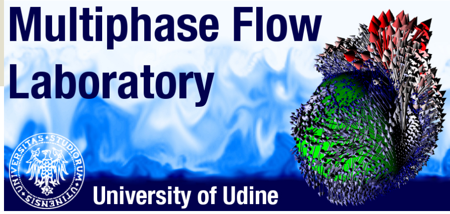

Effect of particle elongation on preferential segregation

Dilute suspension of small rigid fibers in a turbulent channel (Re_τ=300)

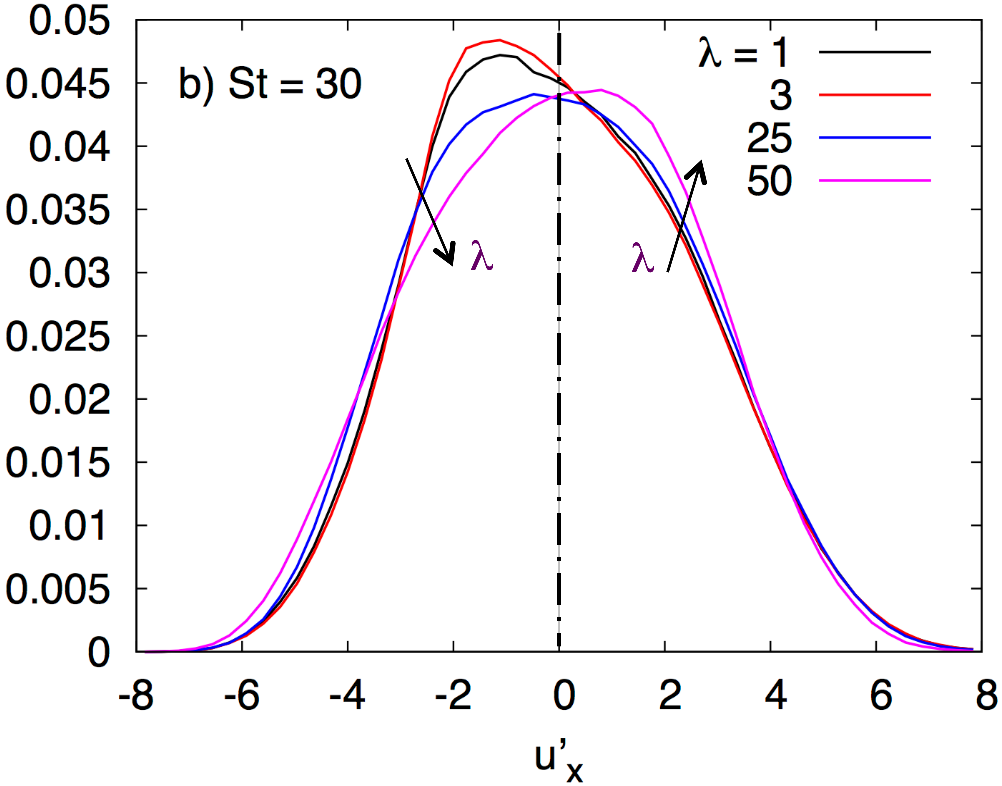

Effect of elongation on near-wall segregation

Instantaneous fiber distribution in the near-wall region

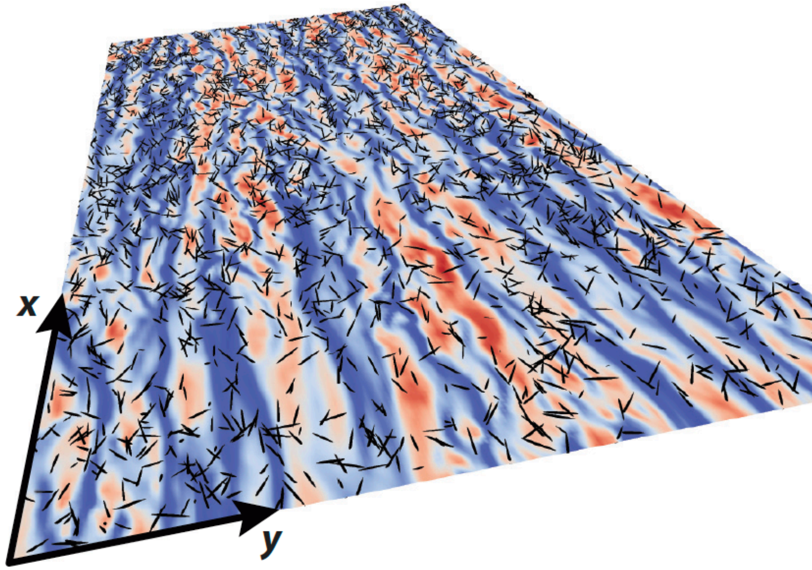

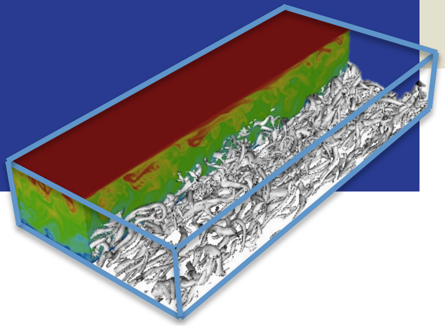

Example of collective behaviour

Flexible fibers in TCF

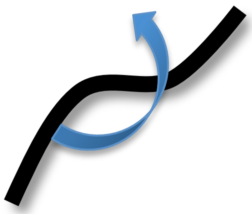

$\mathbf{x}(t,\lambda)$, $\mathbf{v}(\mathbf{x}(t,\lambda),t,\lambda)$, $\omega(\mathbf{x}(t,\lambda),t,\lambda)$, $\mathbf{o}(\mathbf{x}(t,\lambda),t,\lambda)$, $\psi(\mathbf{x}(t,\lambda),t,\lambda)$

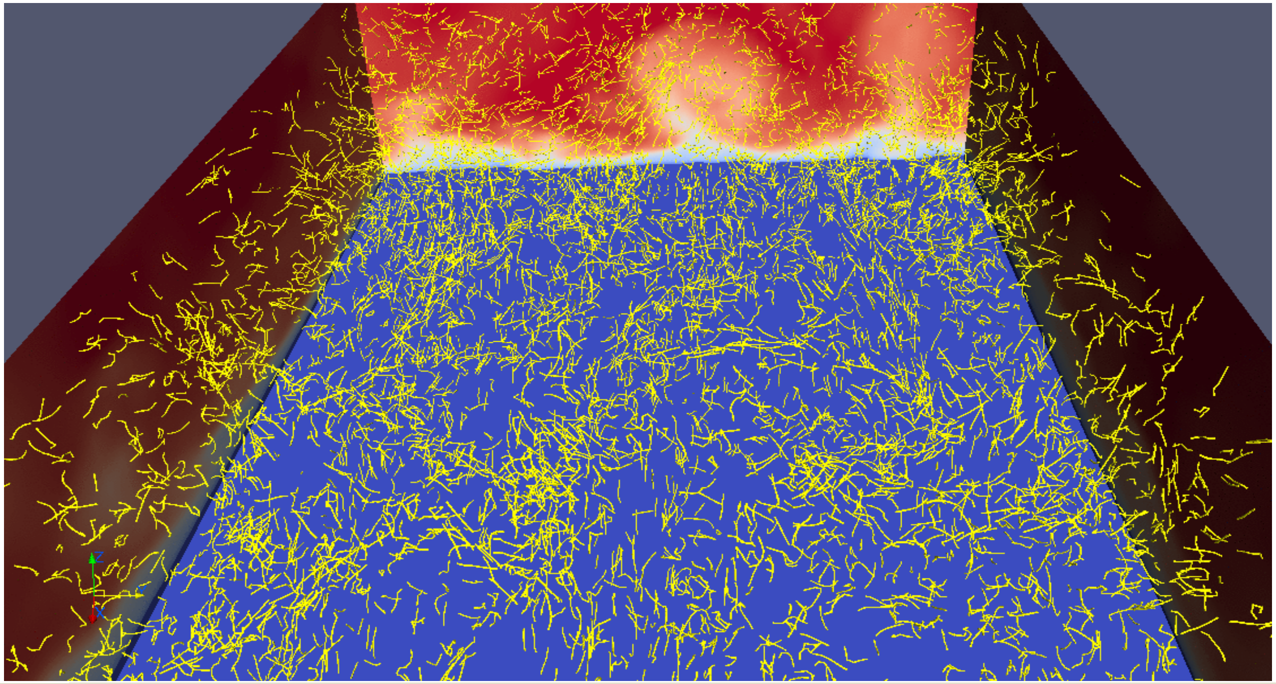

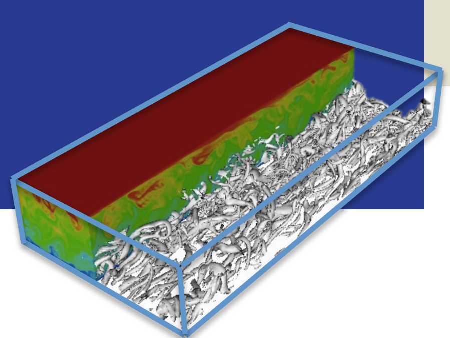

Modelling flexibility: How to "mimic" a flexible fiber?

Rod model: flexible fiber = chain of segments/spheres connected by ball-and-socket joints (Delmotte et al '15; Andric et al '13; Slowicka et al '13; Derksen '10; Lindstrom & Uesaka '07)

- Solve for Euler's 1st and 2nd law for each segment:

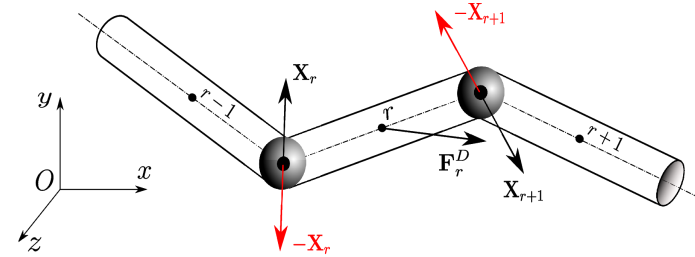

$$m_p \frac{d\mathbf{v}_r}{dt} = \mathbf{F}_r^D + (\mathbf{X}_{r+1} - \mathbf{X}_r)$$

$$\frac{d\left(\bar{\bar{\mathbf{J}}}_r \boldsymbol{\omega}_r\right)}{dt} = \mathbf{T}_r^D + \mathbf{H}_r^D + l\mathbf{o}_r \times (\mathbf{X}_{r+1} + \mathbf{X}_r) + \left(\mathbf{Y}_{r+1}^b - \mathbf{Y}_r^b\right)$$

- Impose connectivity constraints between segments:

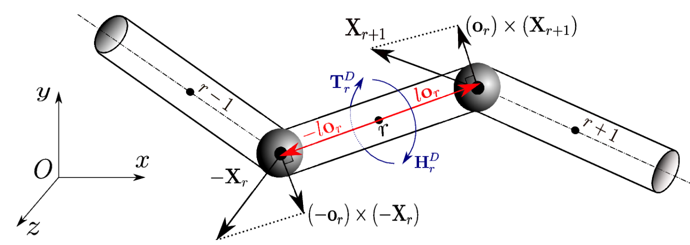

$$\begin{cases} \dfrac{\partial \boldsymbol{\Psi}_r}{\partial t} = \mathbf{v}_{r+1} - \mathbf{v}_r + \lambda a \left(\boldsymbol{\omega}_r \times \mathbf{o}_r + \boldsymbol{\omega}_{r+1} \times \mathbf{o}_{r+1}\right) = \mathbf{0} \\[2em] \boldsymbol{\Psi}_r|_{t=0} = \mathbf{0} \qquad \qquad \boldsymbol{\Psi}_r = \mathbf{p}_r + l\mathbf{o}_r - (\mathbf{p}_{r+1} - l\mathbf{o}_{r+1}) = \mathbf{0} \end{cases}$$

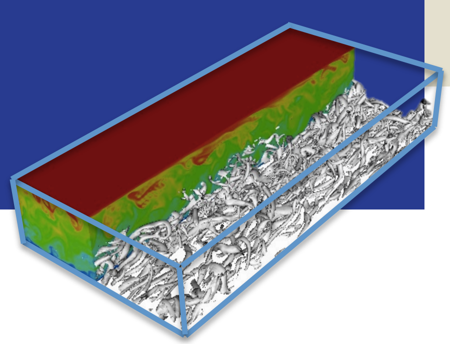

Near-wall accumulation of flexible fibers in turbulent channel flow

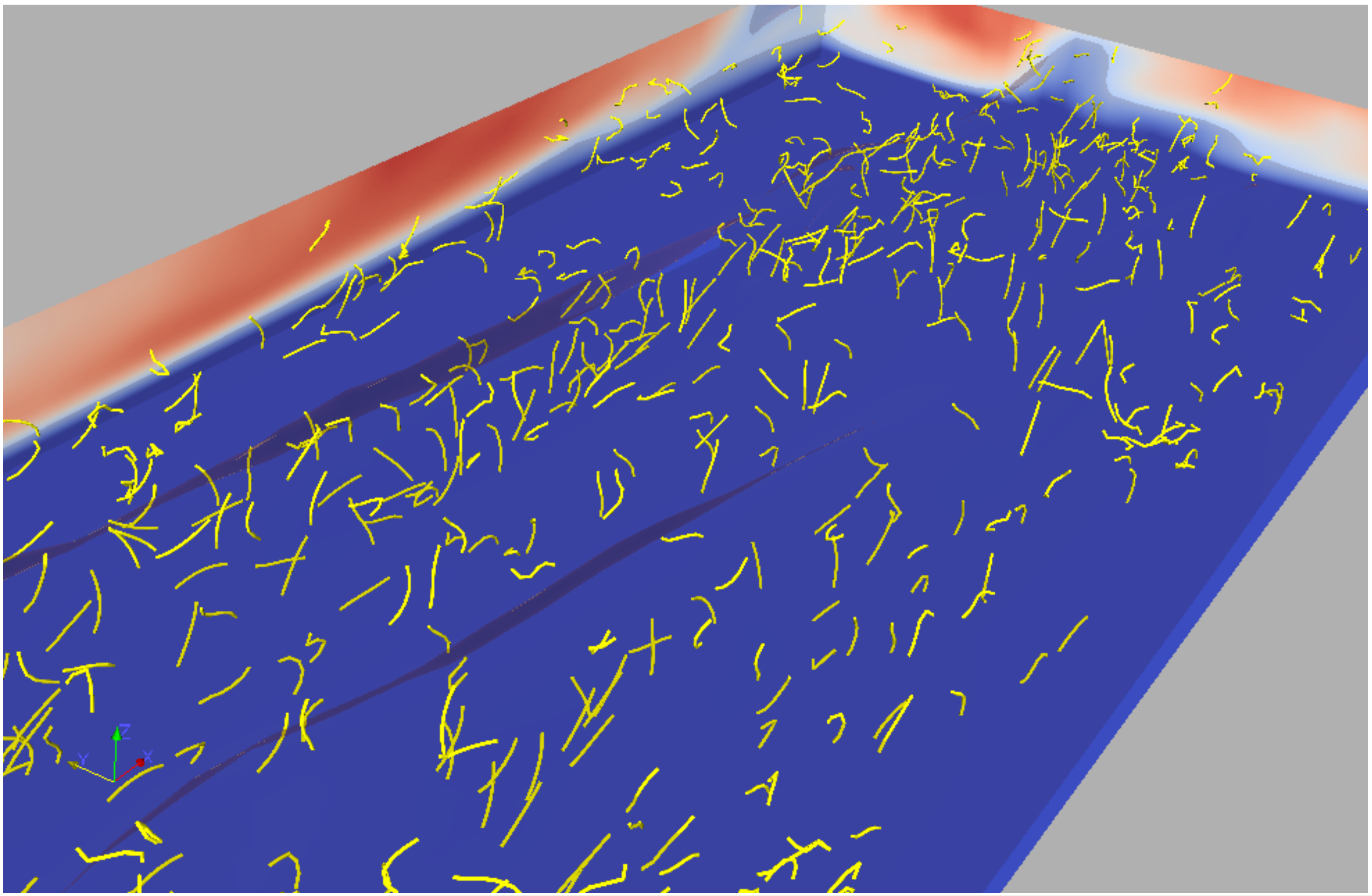

Dilute suspension of small flexible fibers in turbulent channel flow

- Shear Reynolds number: Re_τ=150
- Segment Stokes number: St_s=5, 30
- Segment aspect ratio: λ=5
- Number of segments: 7
- Number of fibers: 200,000

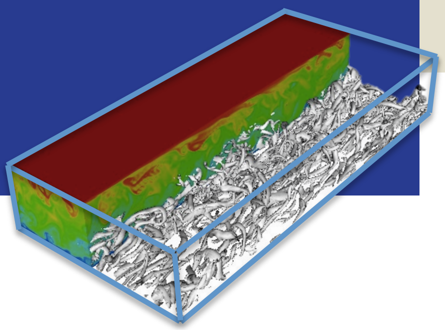

Near-wall accumulation of flexible fibers in turbulent channel flow

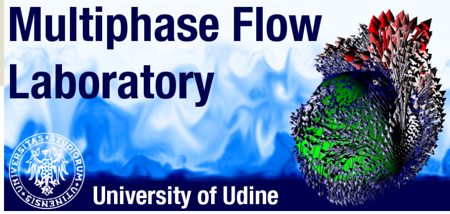

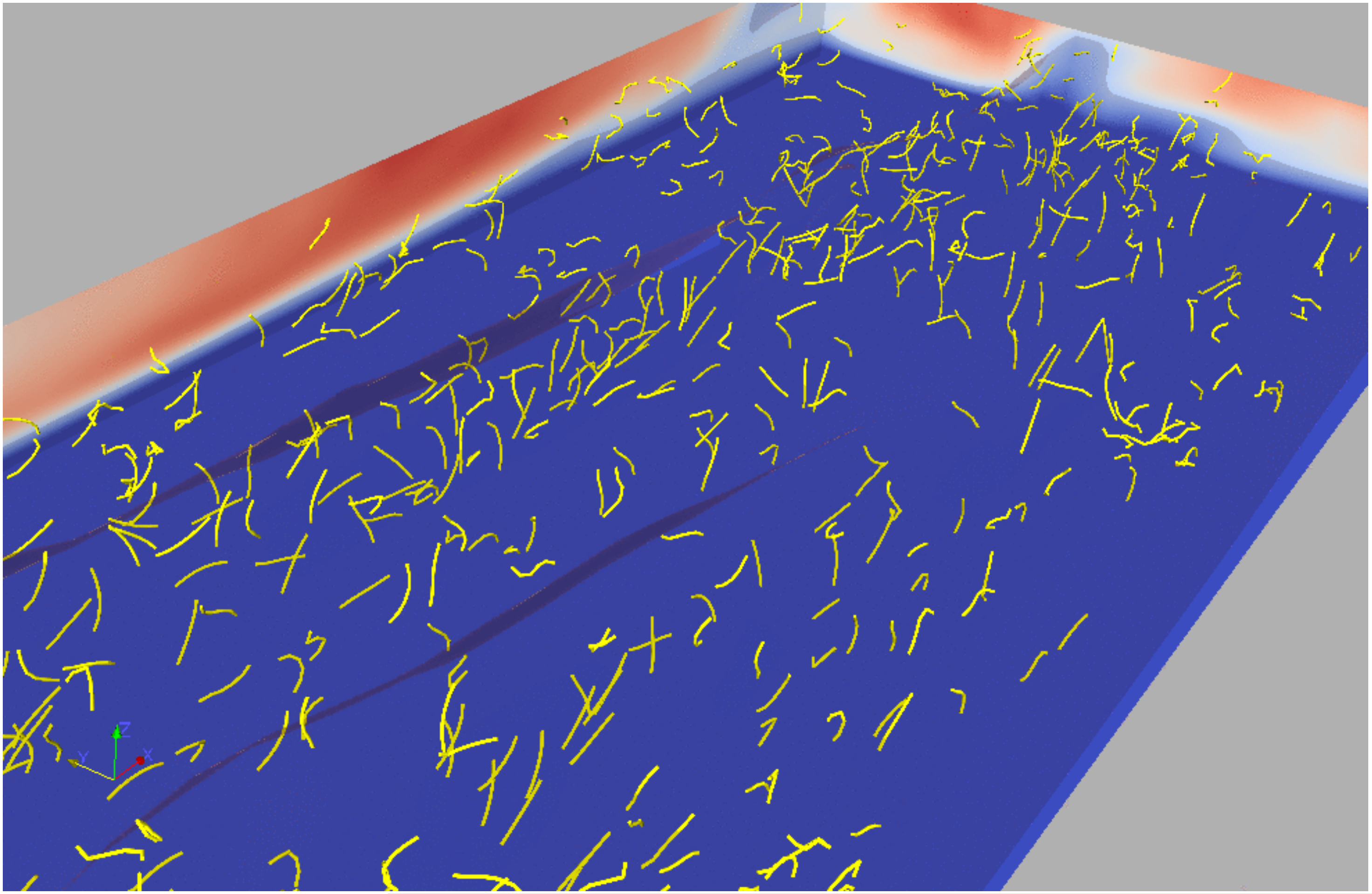

Dilute suspension of small flexible fibers in turbulent channel flow

- Shear Reynolds number: Re_{τ}=150
- Segment Stokes number: St_s=5, 30
- Segment aspect ratio: λ=5
- Number of segments: 7
- Number of fibers: 200,000

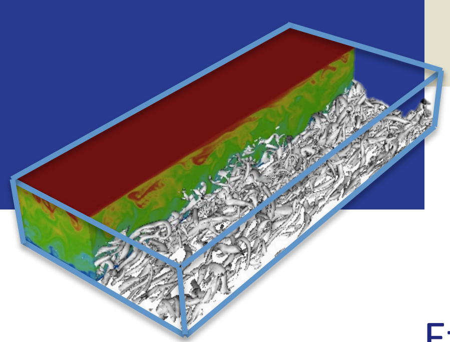

Near-wall accumulation of flexible fibers in turbulent channel flow

Effect of flexibility on near-wall segregation (for $St_s=30$)

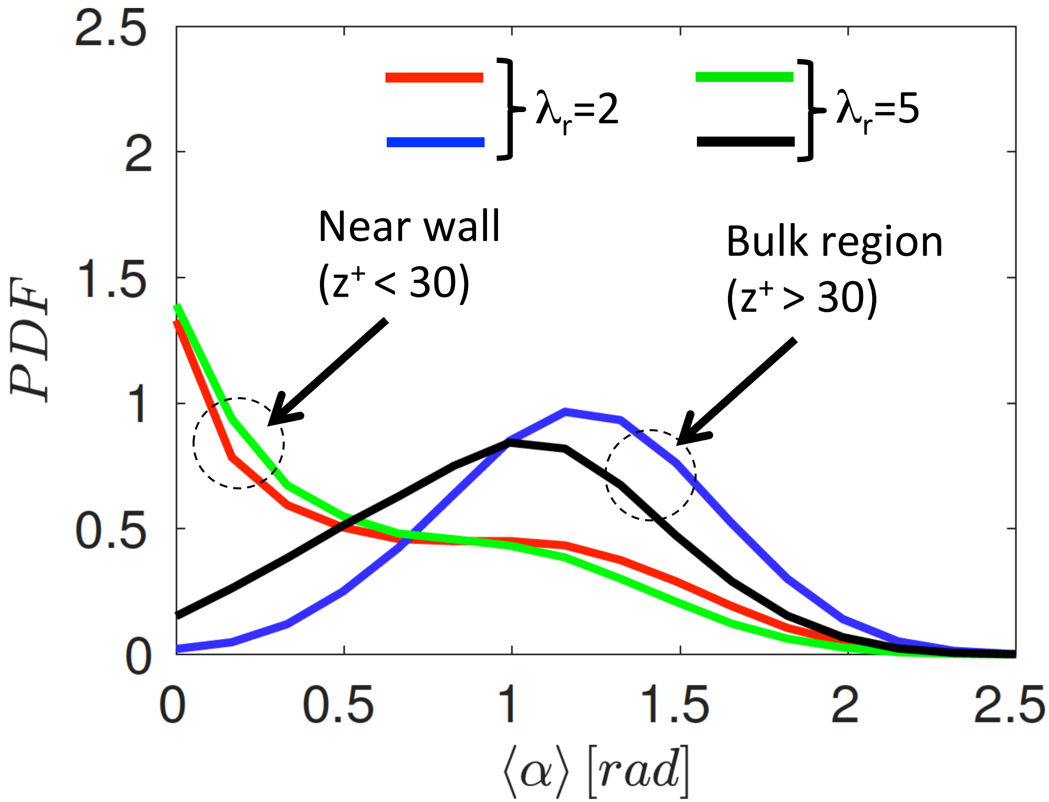

PDF of relative orientation between neighboring fiber elements

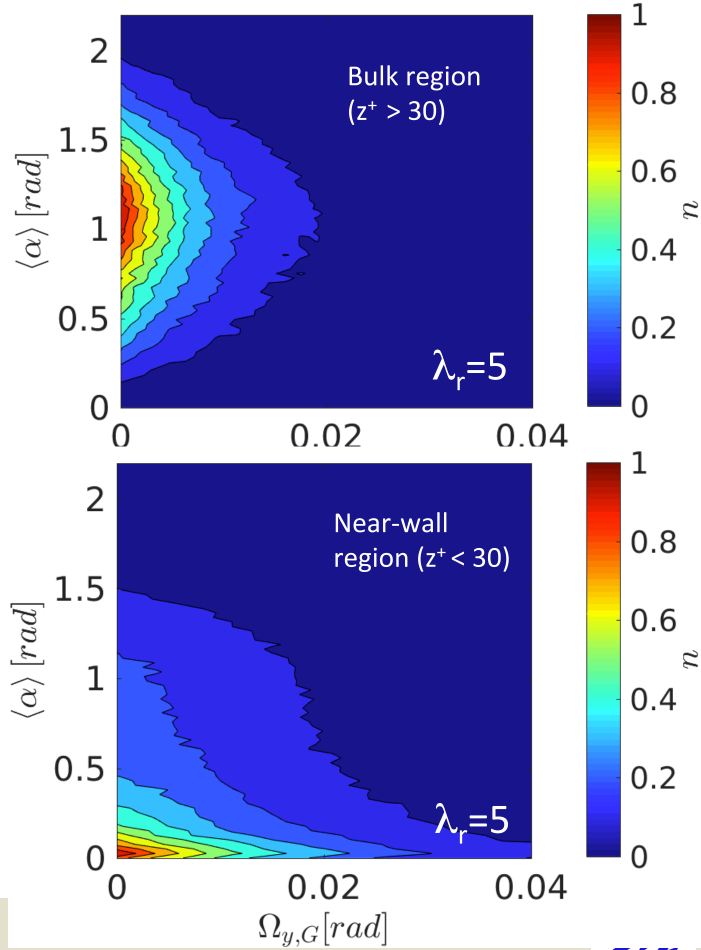

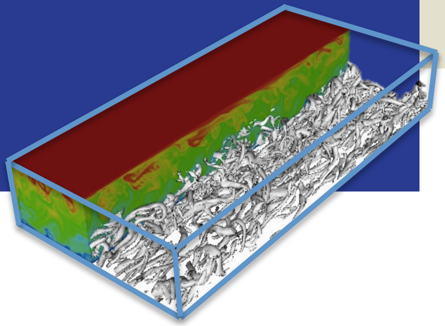

Constraint force acting on fiber elements (along element's axis)

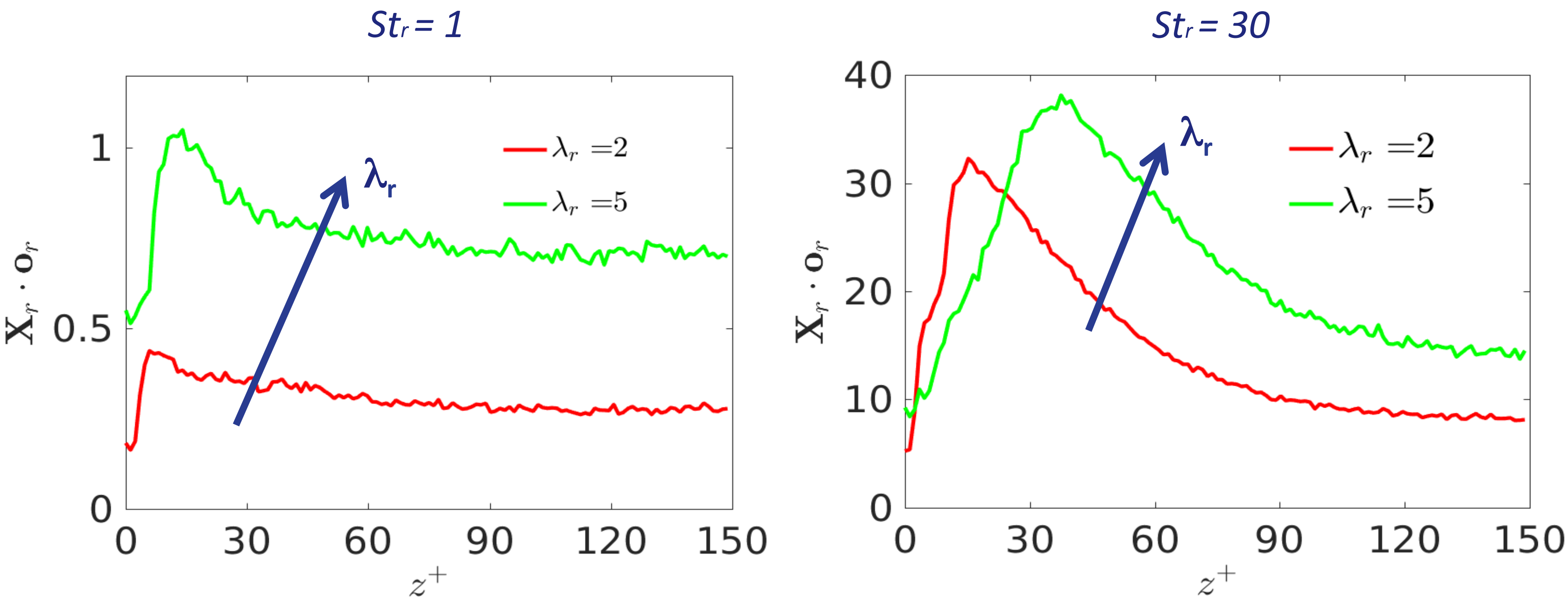

Tensile constraint force as a function of the wall-normal flow direction

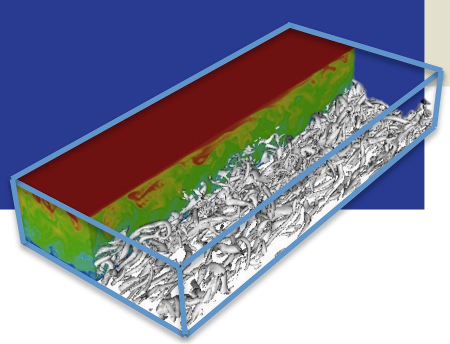

Constraint force acting on fiber elements (perpto element's axis)

$St_r = 1$

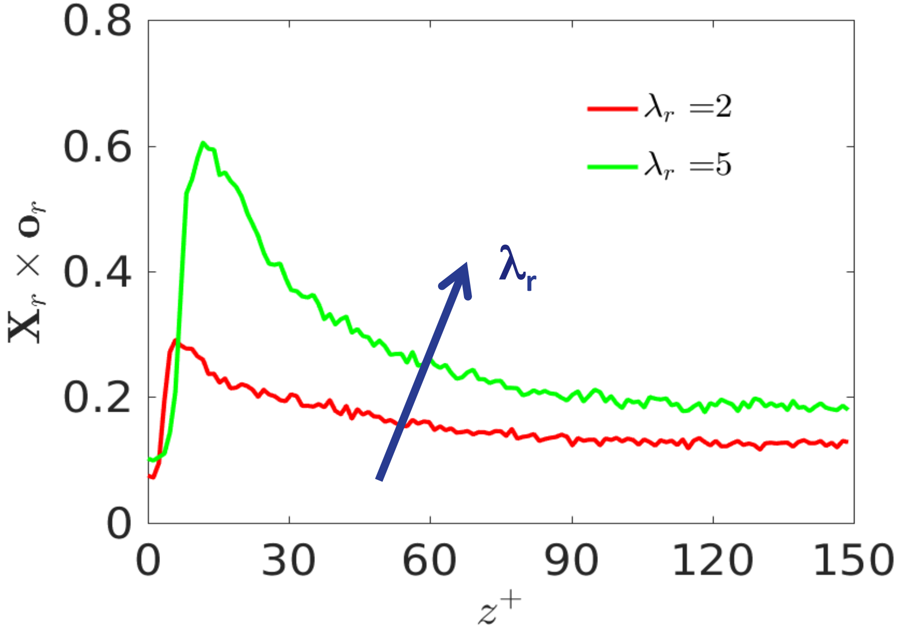

$St_r = 30$

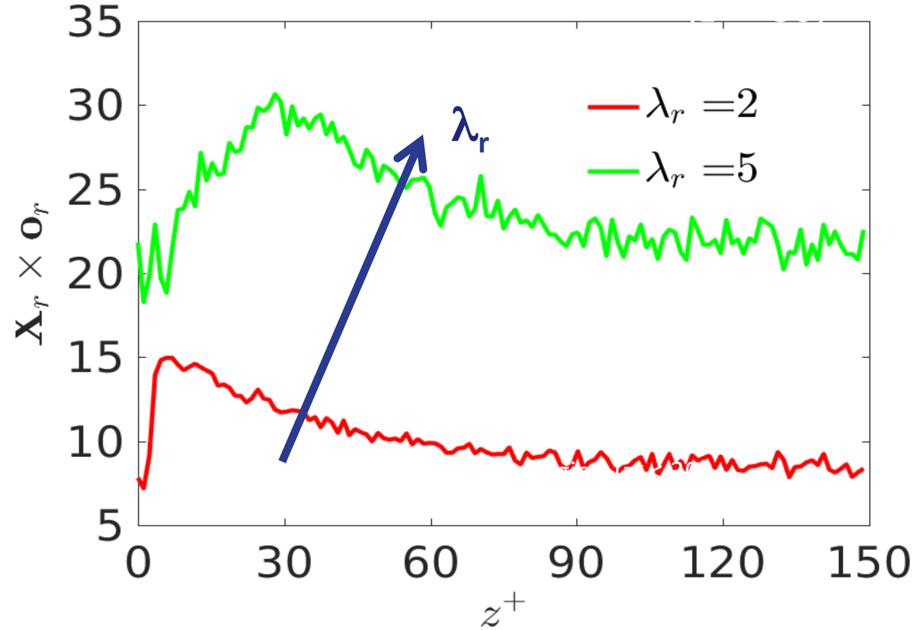

Bending constraint force along the wall-normal flow direction

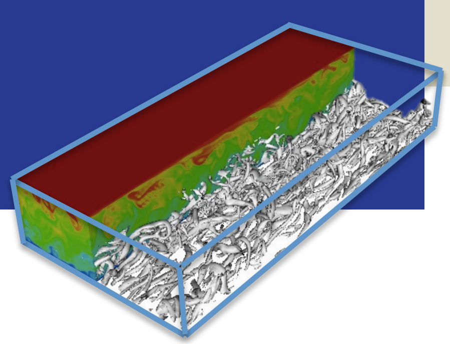

Lessons learned

L1. A Lagrangian framework for numerical simulation of spherical/non-spherical particles dynamics (in dilute flow conditions) has been presented

L2. Equations for particle translation and rotation were derived for particles with arbitrary shape in the Stokes regime (creeping flow)

L3. The resulting lumped-parameter model provides strong mathematical coupling between translation and rotation (drag and lift depend on particle orientation)

L4. Particle rotation can be conveniently described using the quaternion formalism

L5. Equations yield accurate results if particles are small (limit on aspect ratio) and/or have small slip velocity

L6. Many modelling issues remain open (force models, force coupling schemes, torque coupling schemes, collisions, …)